IMPLICATIONS OF AMS-02 MEASUREMENTS WITH UNPRECEDENTED ACCURACY

Yue-Liang Wu

University of Chinese Academy of Sciences (UCAS)
State Key Laboratory of Theoretical Physics (SKLTP)
Kavli Institute for Theoretical Physics (KITPC)
Institute of Theoretical Physics, Chinese Academy of Sciences(ITP, CAS)

AMS DAYS at CERN 2015

H.B.Jin, Y.L.Wu, Y.F.Zhou, arXiv:1410.0171, to appear in JCAP
H.B.Jin, Y.L.Wu, Y.F.Zhou, JCAP 1311, 026 (2013)
Z.P.Liu, Y.L.Wu, Y.F.Zhou, PRD 88, 096008 (2013）

AMS-02 new results in 2014 was selected by the members of CAS & CAE as the 2014 world-wide top 10 news in sciences & technology ;

阿尔法磁谱仪项目最新研究成果被中国两院院士评选为2014年国际十大科技新闻

美籍华人物理学家丁肇中9月18日公布阿尔法磁谱仪项目最新研究成果，进一步显示宇宙射线中过量的正电子可能来自暗物质。根据研究小组在《物理评论快报》上发布的数据，阿尔法磁谱仪观察到的410亿个宇宙射线事件中，约有1000万个是电子或正电子。正电子似乎来源于宇宙空间的各个方向，而不是某个特定方向。研究人员说，观测到的正电子分布特征与暗物质理论的某个模型一致，该模型认为暗物质由一种称为“中轻微子”的粒子组成。

CAS President Prof. C.L. Bai awarded Prof. S.Ting a honorary professor of UCAS

40 Years on Discovery of J Particle (Charm Quark)

"New Results of AMS-02" talk by Prof. S.Ting at UCAS in 2014

OUTLINE

- **Introduction**
  - On DM
  - Latest AMS-02 results
  - CR propagation in the Galaxy
- **Implications of AMS-02 Results with Unprecedented Accuracy (I)**
  - **CR propagation models with selected CR parameters**
  - **DM annihilation and decay**
- **Implications of AMS-02 Results with Unprecedented Accuracy (II)**
  - **Constraining more stringently CR propagation models by using AMS-02 data**
    - Based on B/C ratio and proton flux
    - Determination on the propagation parameters
    - Uncertainties in backgrounds
  - **Predictions and uncertainties for the DM annihilations**
    - Positrons and electrons
    - antiproton fluxes from DM
  - **Predictions and uncertainties for the CR antiprotons**
    - Upper limits on antiproton flux from PAMELA data
    - Projections for the AMS-02 antiproton results
      - mock data of AMS-02 three-year data taking
      - Reconstruction capability

Mechanisms for boost factor to explain AMS02 data with DM

ASTRONOMICAL EVIDENCES ON EXISTENCE OF DARK MATTER

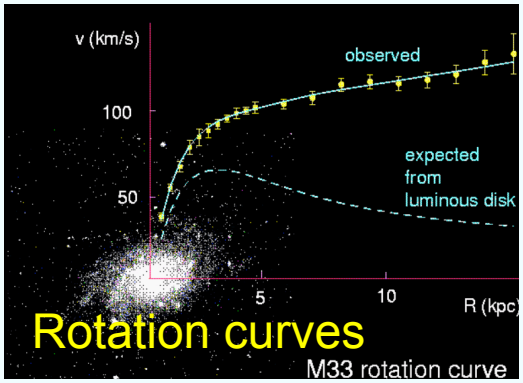

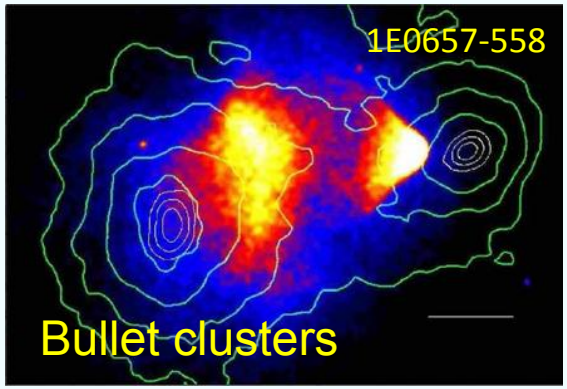

Tucker,etal, APJ,496,L5(1998)

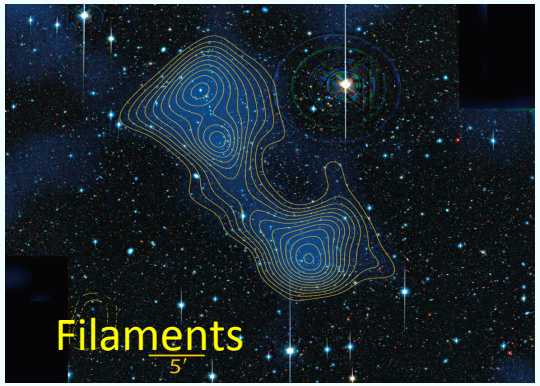

J.P. Dierich etal, 1207.8089, Nature

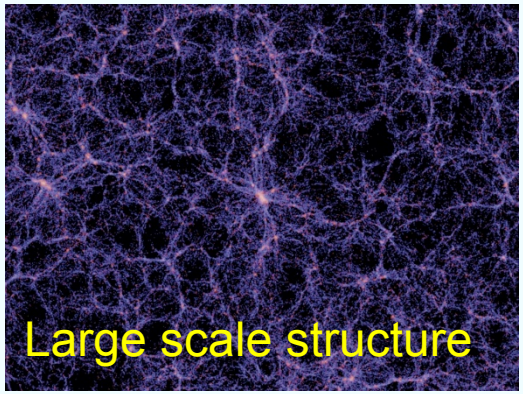

Millennium Simulation

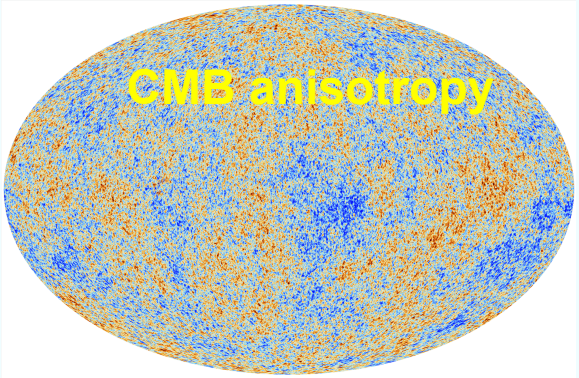

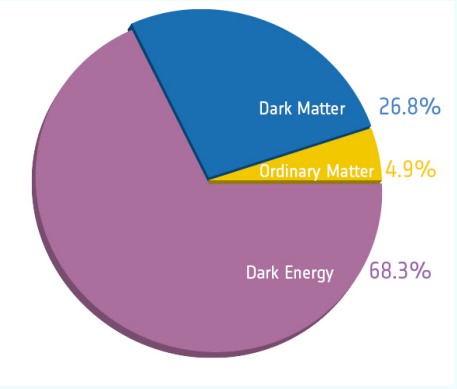

Planck, arXiv:1303.5062

There are various evidences on the existences of dark matter, While its nature remains unknown!

Weakly Interacting Massive Particles (WIMPs)

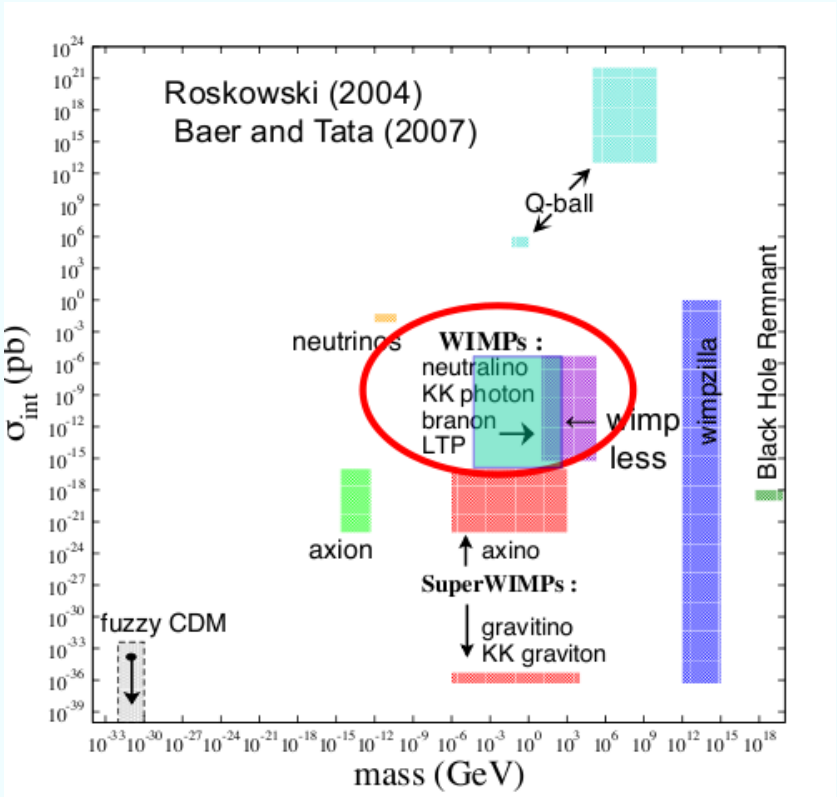

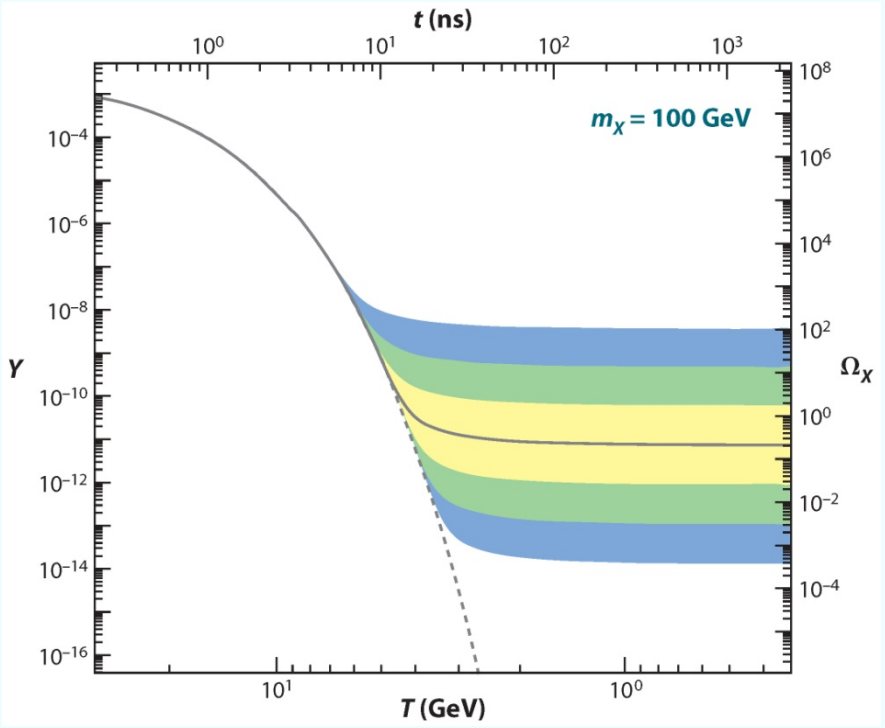

$$\Omega h^2 \approx -\frac{3 \times 10^{-27} \mathrm{cm}^3 \mathrm{s}^{-1}}{< \sigma v >}$$

Weakly Interacting Massive Particles (WIMPs)

- Particle physics naturally predicts WIMPs
- WIMPs have just the right thermal relic density
- WIMPs are testable by the current exp.

Detecting the WIMPs

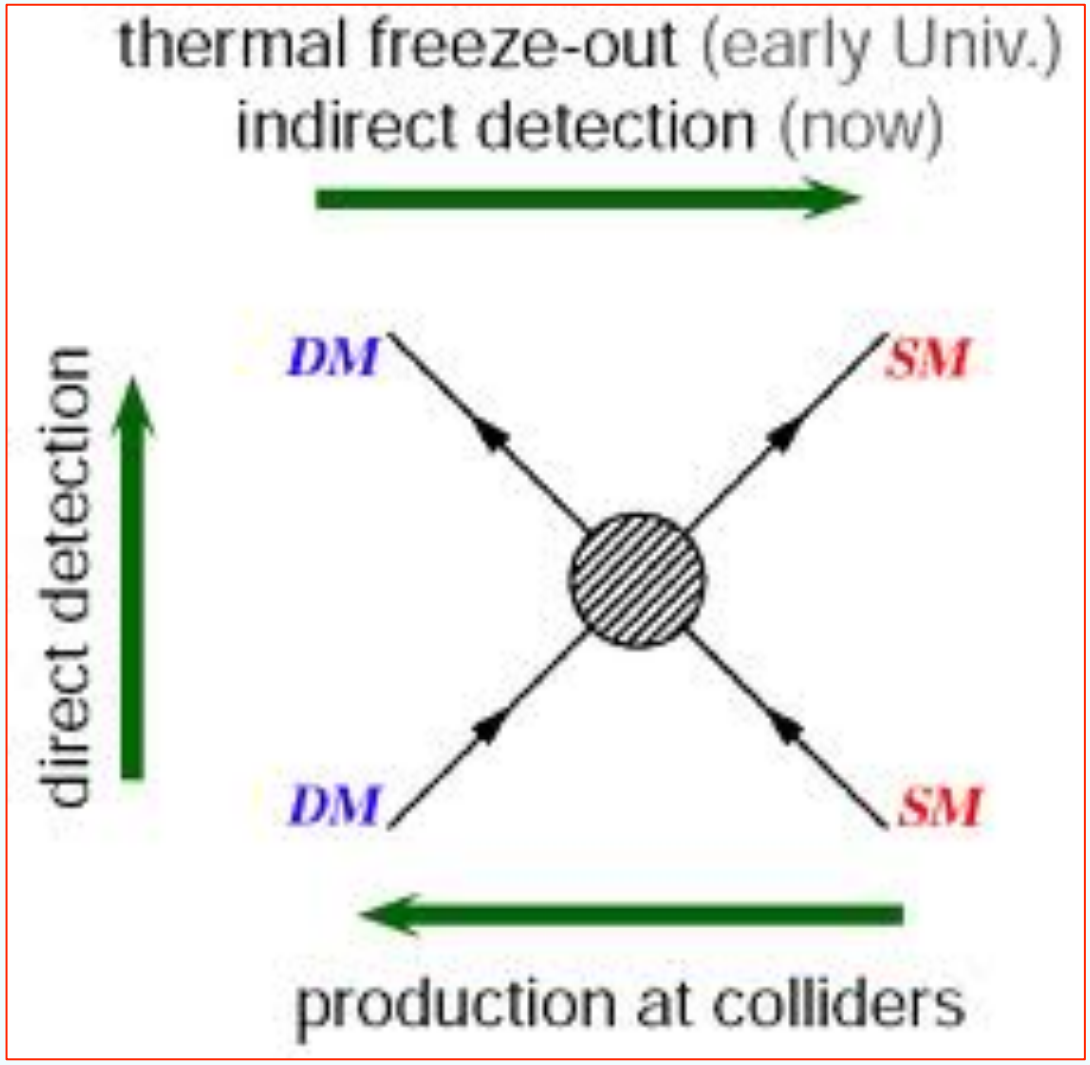

DM Direct Detection

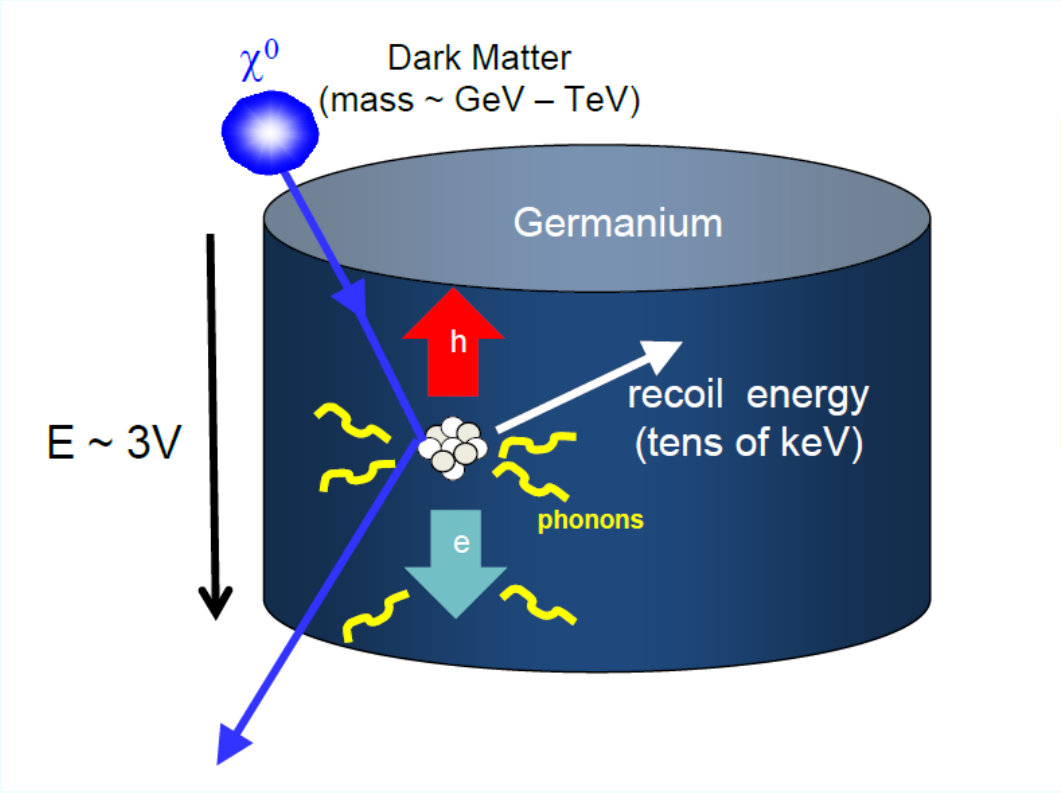

There are no confirmed evidences on WIMPs as DM from the direct detections so far.

DM-Nucleon Scatterings

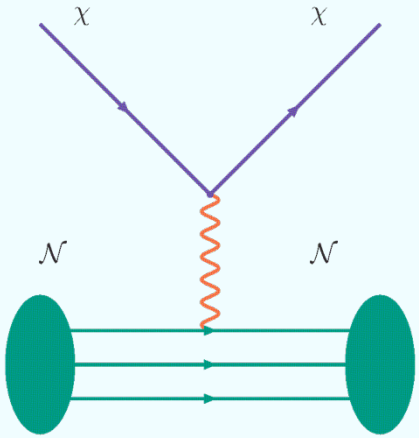

Particle phys.

$$R = N_T \left(\frac{\rho_0}{m_\chi}\right) \frac{m_A \sigma_0}{2\mu_A^2} \int F^2(E_R) dE_R \int_{v_{min}}^{v_{esc}} d^3v \frac{f(v)}{v},$$

astrophysics | Nuclear phys. | astrophysics

Theoretical assumptions commonly adopted

- **Smooth local DM energy density (ρ=0.2-0.7 GeV/cm^3)**
- **Contact interactions (heavy mediator, no q^2 and v-dependences)**
- **Elastic scatterings**
- **Isospin-conserving interactions (for Spin-independent cross-section)**
- **Form factors (Helm etc.)**
- **Velocity distribution of halo DM (Maxwellian-Boltzmann)**

Experimental uncertainties that may change interpretation of data

- Backgrounds, surface vs. bulk event …
- Quenching factors/scintillation efficiencies
- Energy resolution/thresholds

DM Production at Colliders

Mono-jet, -photon, -*Z*, -*W*, -quark and lepton + missing E_T

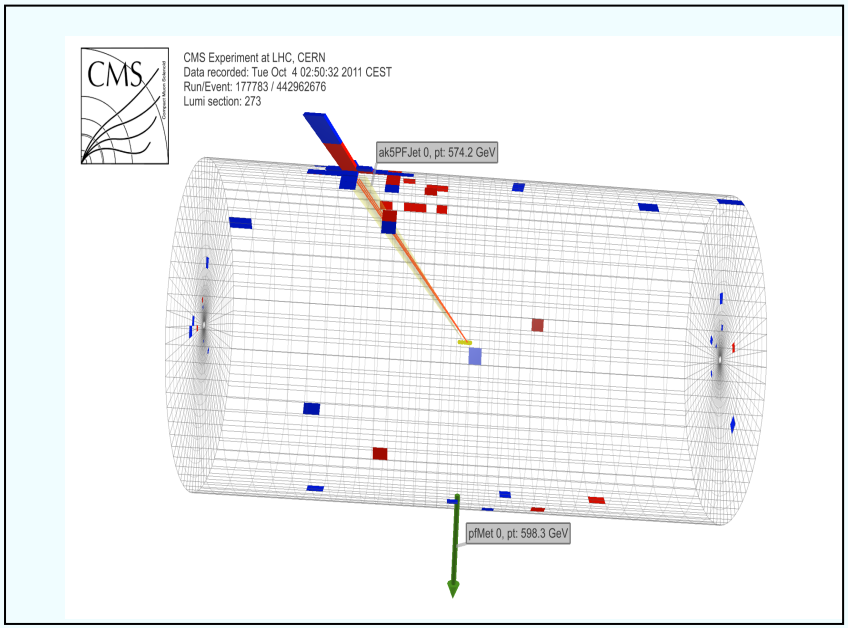

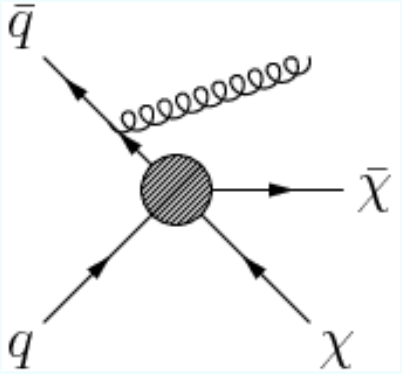

(a) $q\bar{q} \to \chi\chi + g$

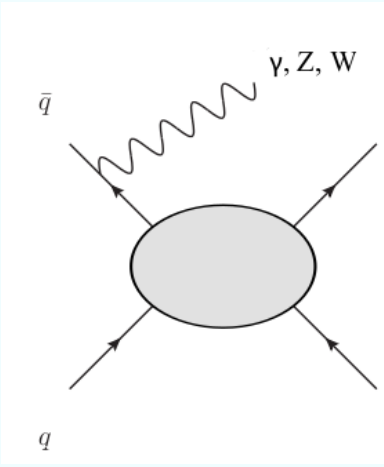

(b) $q\bar{q} \to \chi\chi + \gamma, Z, W$

There is no signal on WIMPs as DM from LHC so far

LHC: mono-jet, -photon,-lepton

Assume effective operators

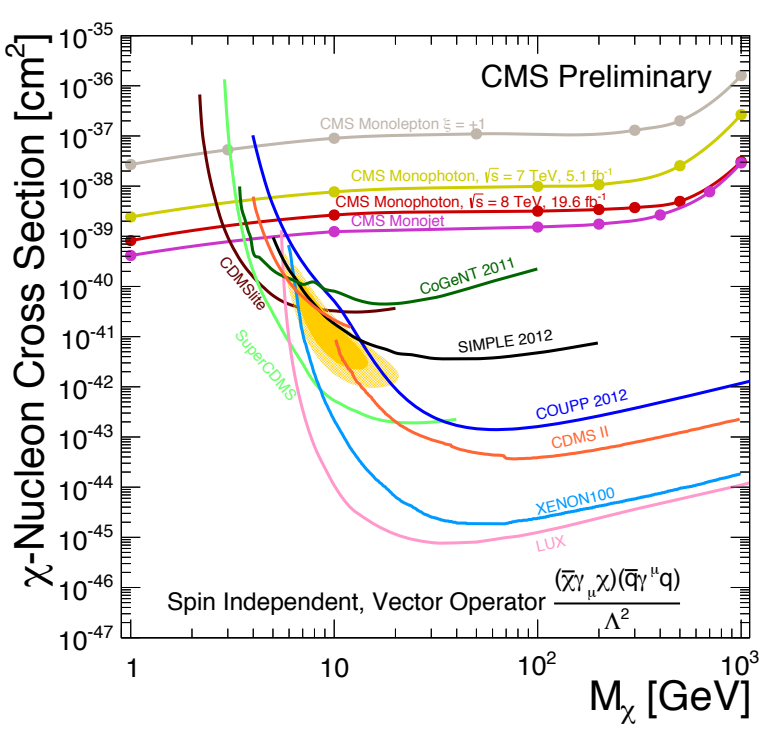

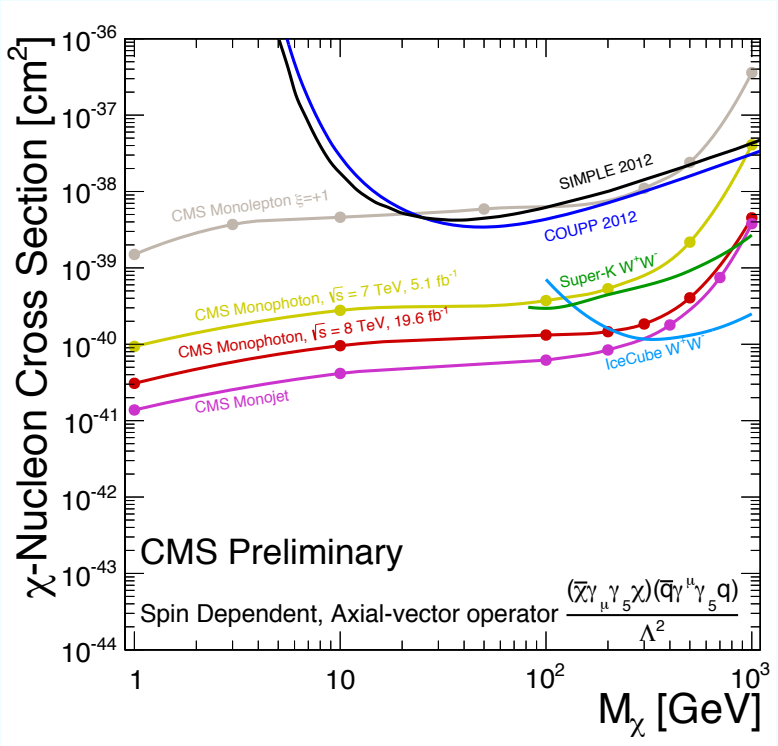

Spin-independent case

Spin-dependent case

CMS, 1410.3762

DM Indirect Detection

AMS-02 Measurements with Unprecedented Accuracy

AMS-02 Positron Fraction (2014)

PRESS RELEASE
AMS Collaboration
CERN, Geneva, 18 September 2014

New results from the Alpha Magnetic Spectrometer on the International Space Station

The new results on energetic cosmic ray electrons and positrons are announced today. They are based on the first 41 billion events measured with the Alpha Magnetic Spectrometer (AMS) on the International Space Station (ISS). These results provide a deeper understanding of the nature of high energy cosmic rays and shed more light on the dark matter existence.

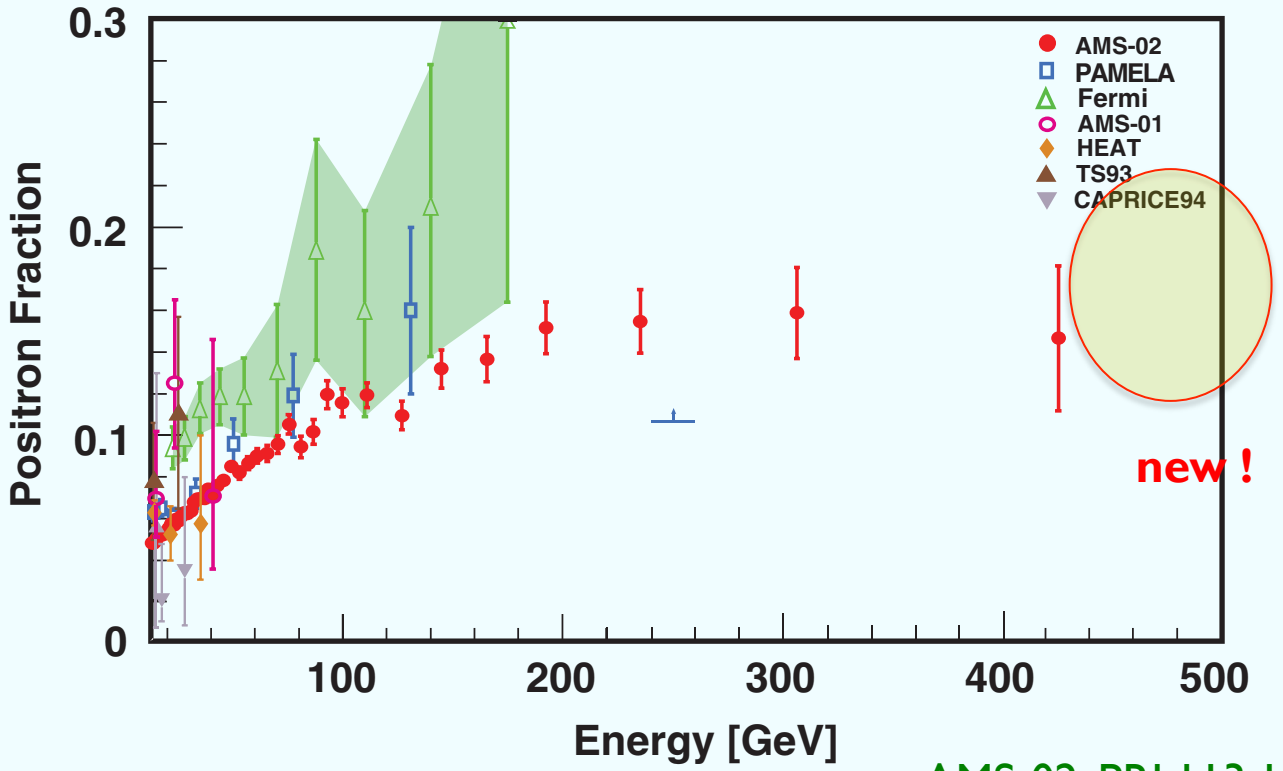

AMS-02, PRL113,121101(2014)

AMS-02 e^- and e^+ Fluxes (2014)

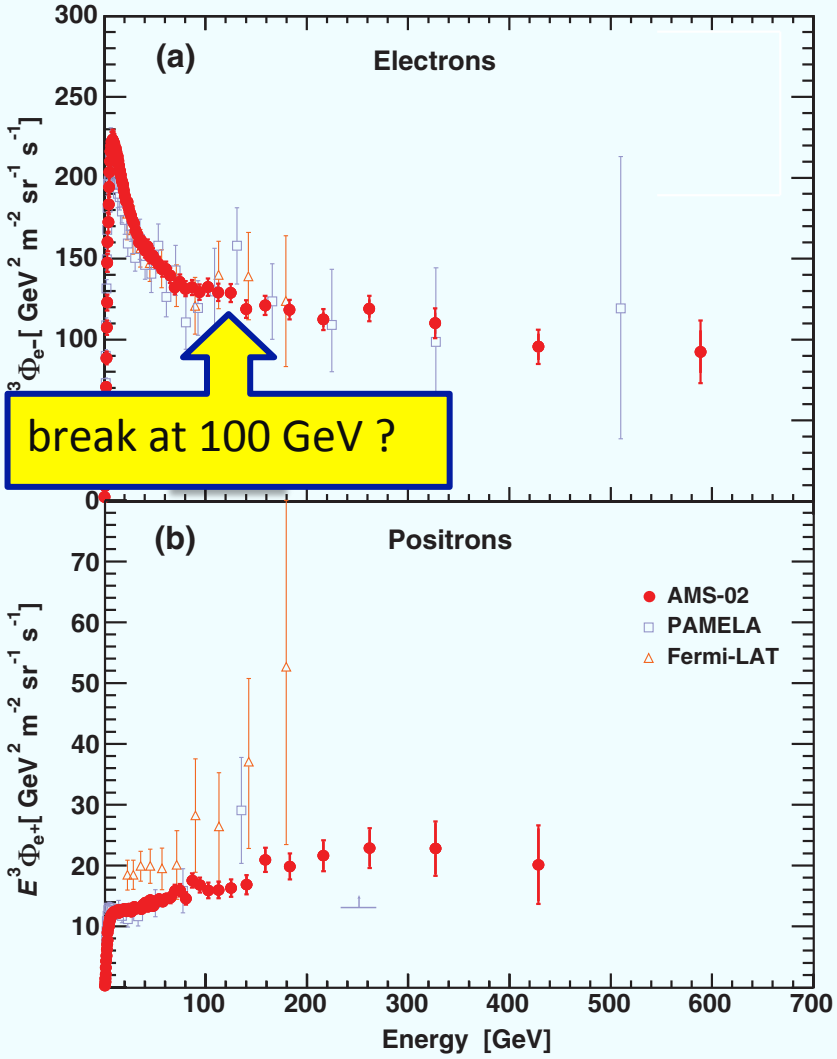

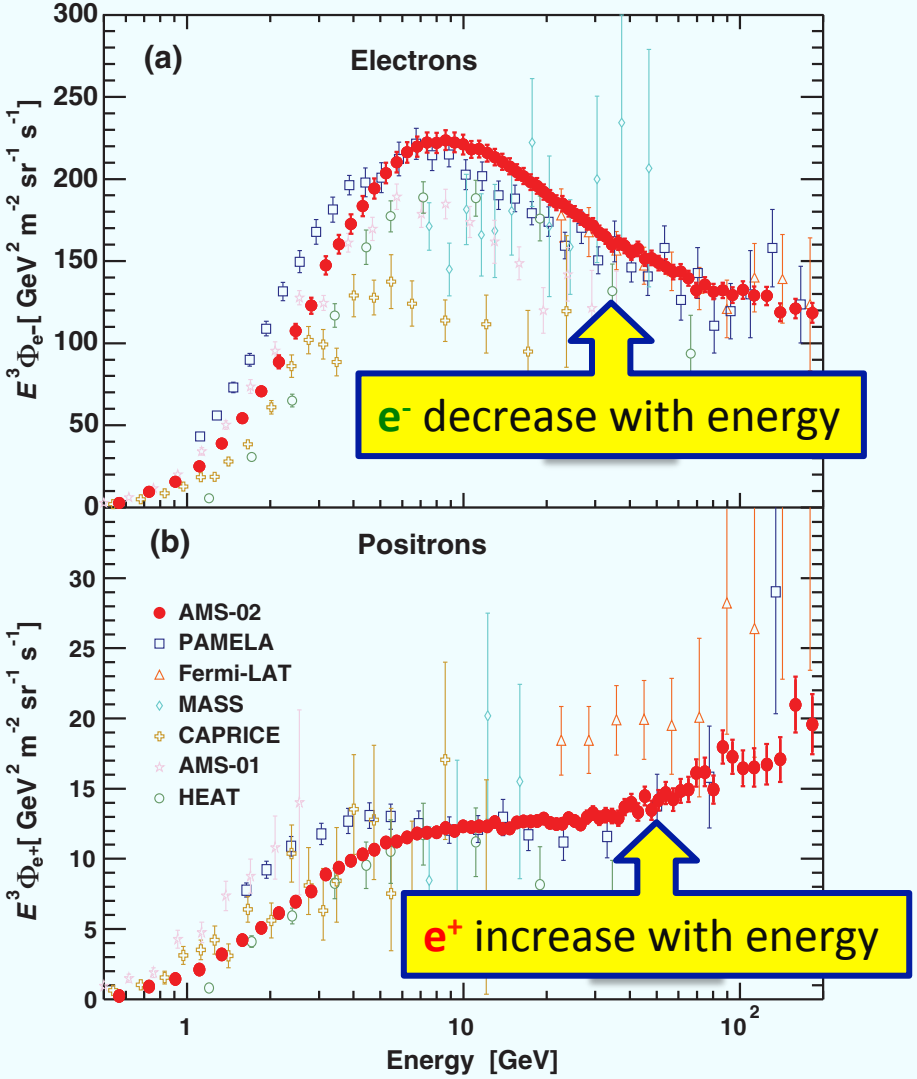

AMS-02, PRL113,121102(2014)

AMS-02 (e^++e^-) Total Flux (2014)

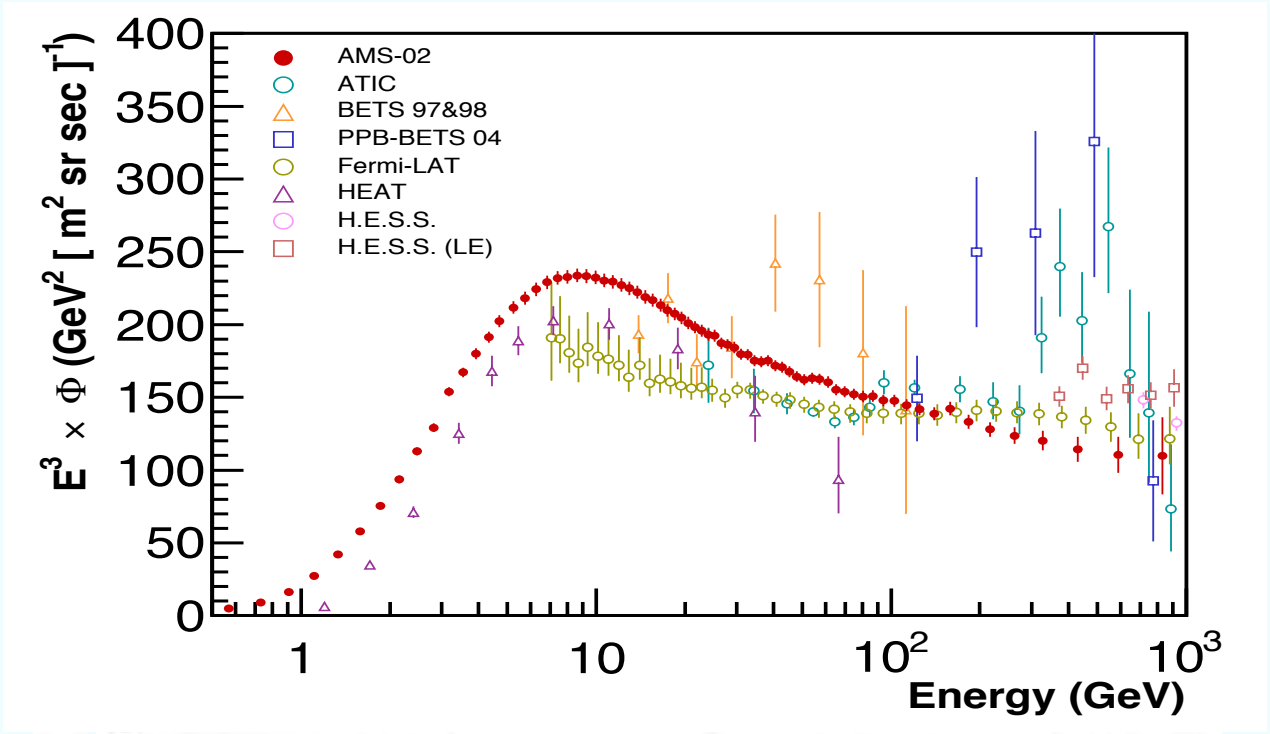

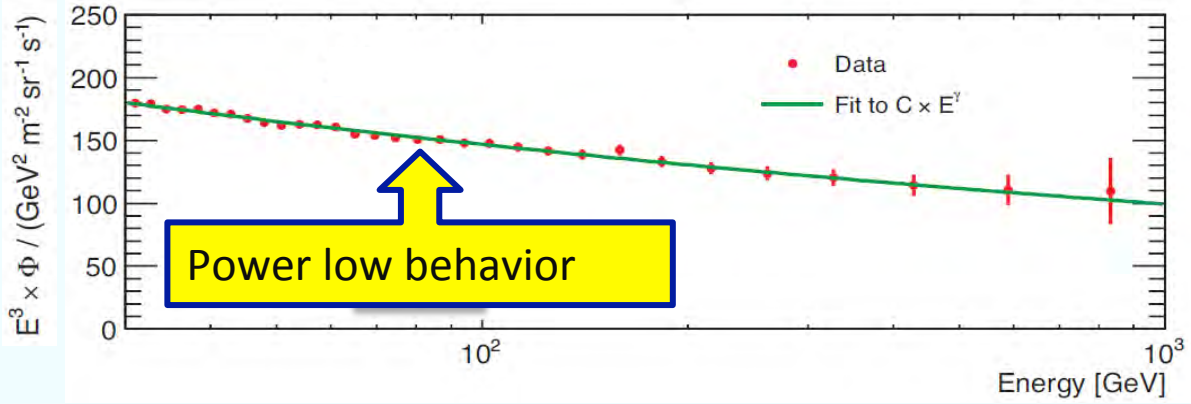

AMS-02 B/C Ratio (2013)

AMS-02, ICRC 2013

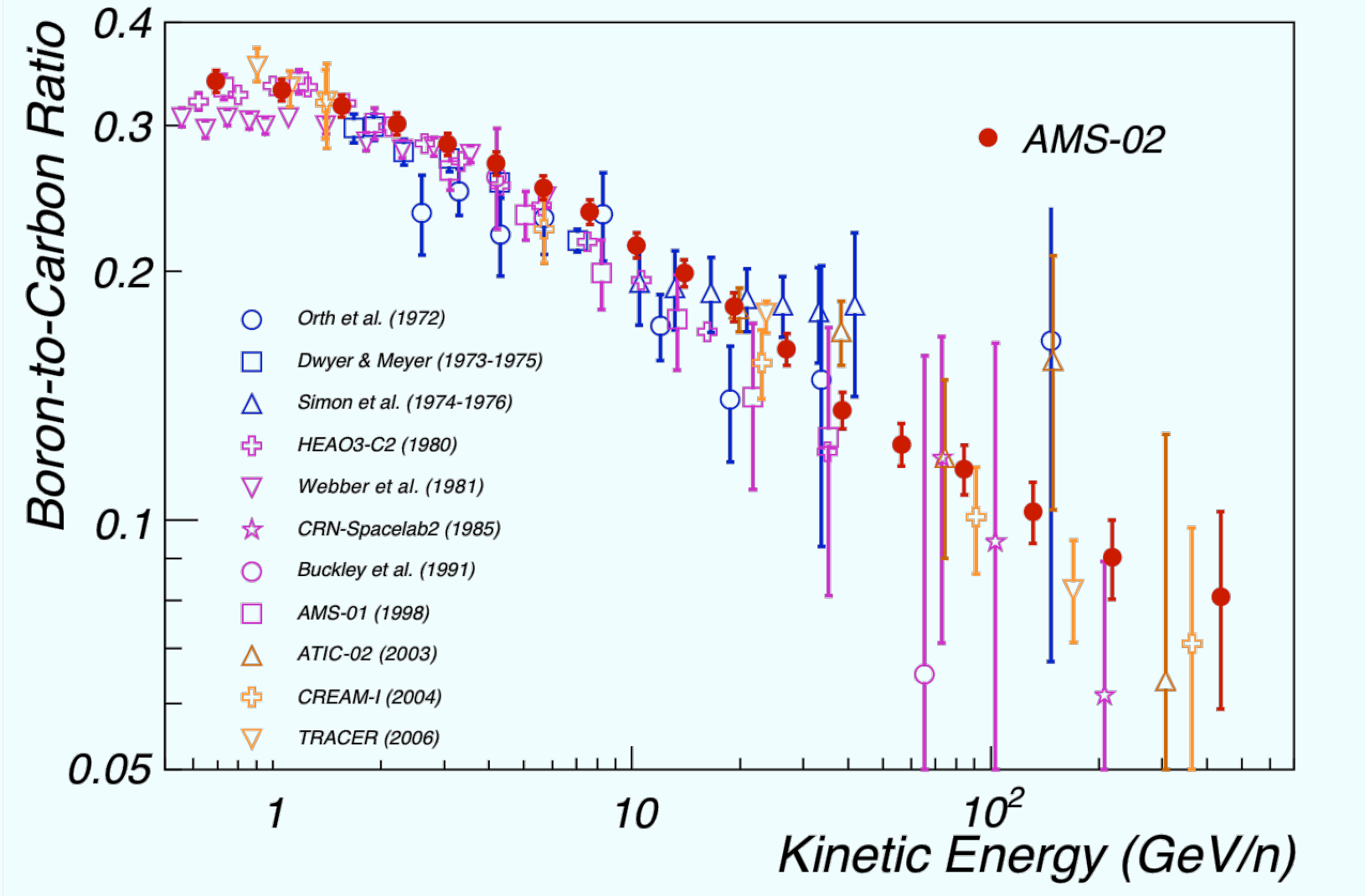

AMS-02 Proton Flux (2013)

AMS-02, ICRC 2013

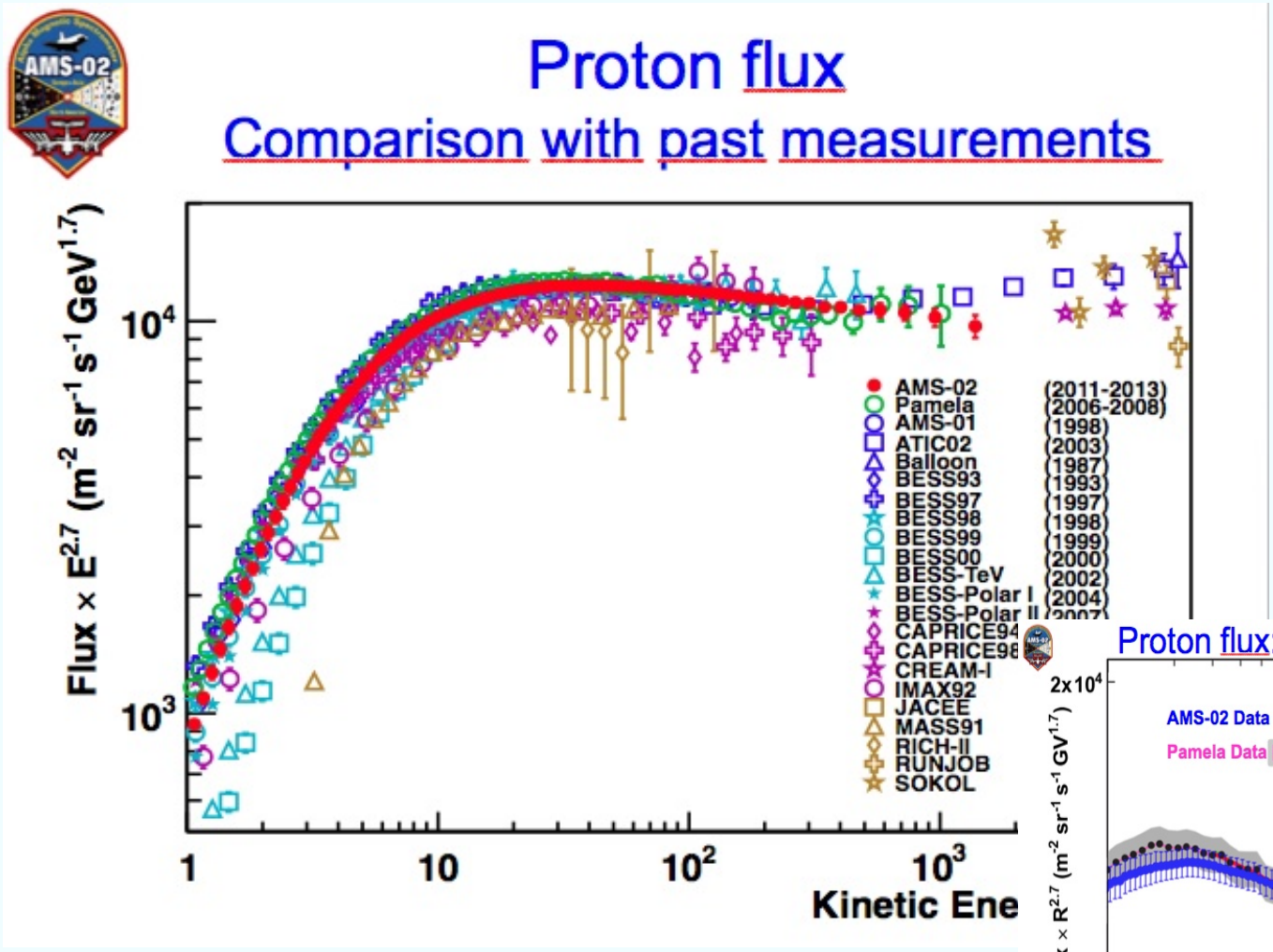

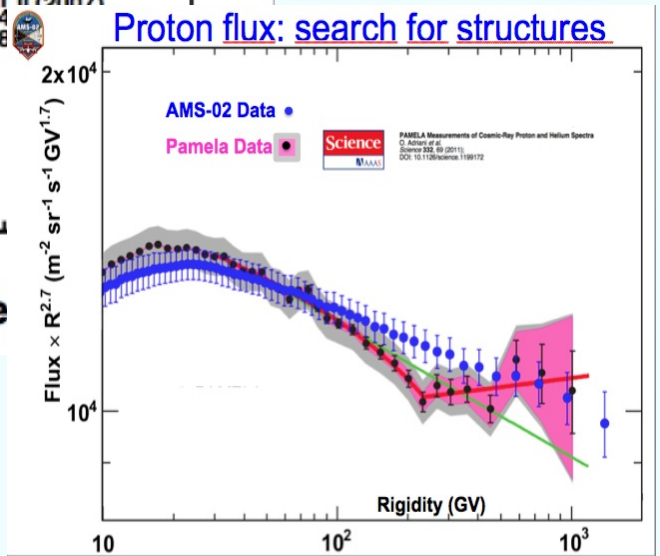

Power law behavior at E >100 GeV

Latest New Results

Reported at ASM Days @ CERN

- **S. Ting** — **Introduction to AMS experiment**
- **A. Kounine** — **Latest AMS results: e+ fraction, pbar/p**
- **S. Schael** — **The e- and e+ spectrum from AMS**
- **B. Bertucci** — **The e+ plus e- spectrun from AMS**
- **V. Choutko** — **The proton spectrum from AMS**
- **S. Haino** — **The Helium spectrum from AMS**
- **A. Oliva** — **AMS results on light nuclei B/C**
- **L. Derome** — **AMS results on light nuclei Li**
- **M. Heil** — **AMS results on light nuclei C/He**

IMPLICATIONS OF AMS-02 RESULTS

Can we more precisely predict the CR spectra?
How to distinguish DM source and astronomical source?

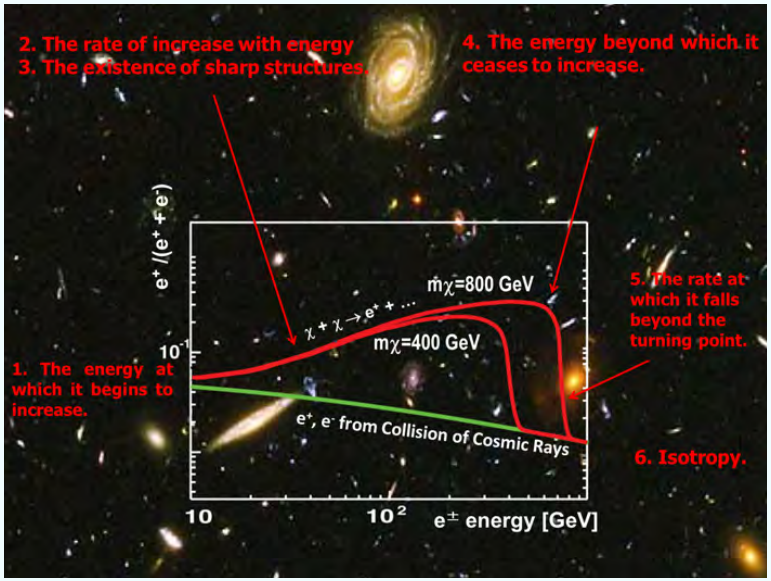

How CRs travel across the Galaxy?

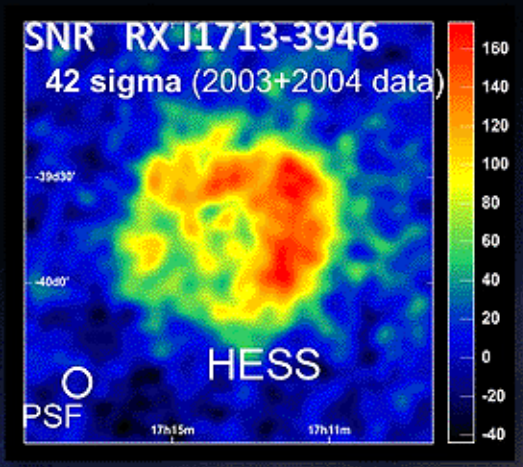

Sources (SNR)

Sources (DM)

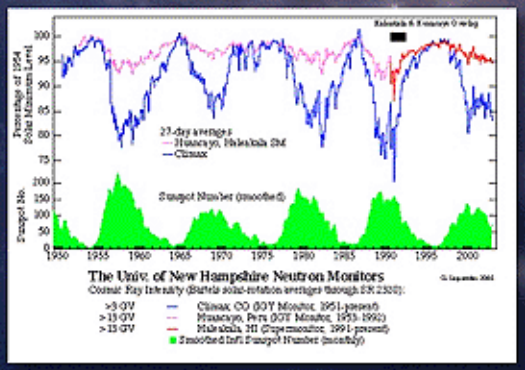

X,γ

e±

P, P̄

X,γ

e±

P
He
CNO

•diffusion
•energy losses
•reacceleration
•convection
•production of secondaries

B

ISRF

gas

synchrotron

IC

bremss

π0

ISM

Detectors

20 GeV/n

PAMELA

e

LiBeB

He

CNO

ACE

helio-modulation

CR species:
- Only 1 location
- Heliospheric modulation

Cosmic Ray Propagation

Diffusion equation for Number density per unit of total particle momentum

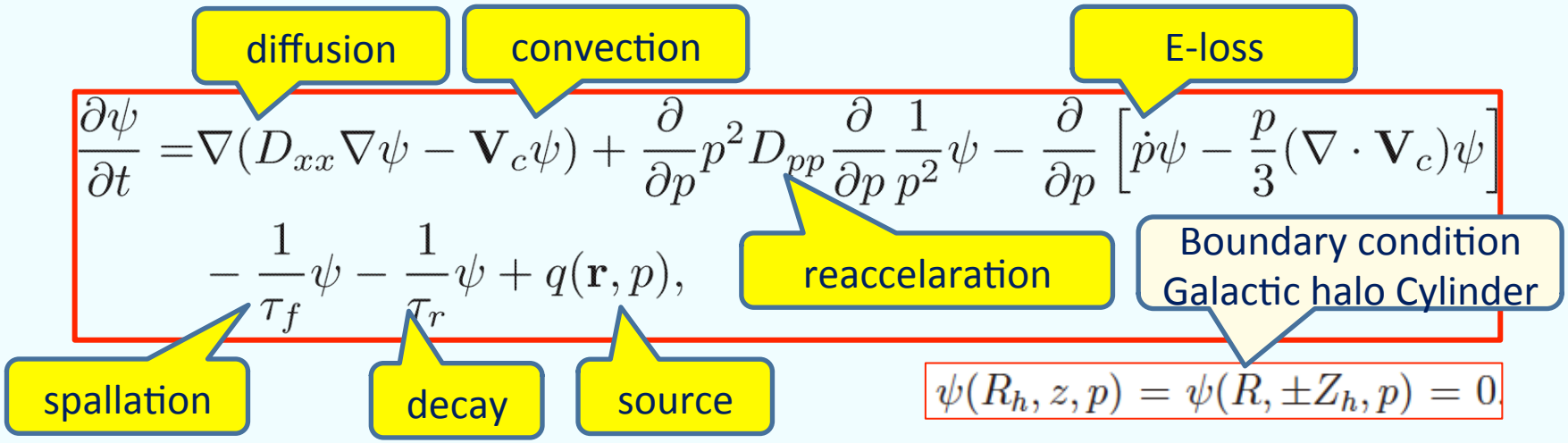

$$\frac{\partial \psi}{\partial t} = \nabla(D_{xx}\nabla\psi - \mathbf{V}_c\psi) + \frac{\partial}{\partial p}p^2 D_{pp}\frac{\partial}{\partial p}\frac{1}{p^2}\psi - \frac{\partial}{\partial p}\left[\dot{p}\psi - \frac{p}{3}(\nabla\cdot\mathbf{V}_c)\psi\right] - \frac{1}{\tau_f}\psi - \frac{1}{\tau_r}\psi + q(\mathbf{r},p),$$

$$\psi(R_h, z, p) = \psi(R, \pm Z_h, p) = 0$$

Processes involved

- Diffusion (magnetic field)
- Convection (galactic wind)
- Reacceleration
- Energy loss
  - Ionization/Coulomb scattering
  - Inverse Compton scattering
  - Synchrotron/bremsstrahlung
  - Adiabatic energy loss due to convection
- Spallation (Fragmentation and interactions)
- Radioactive decay
- Solar modulation

Sources of CR particles

- Primary sources from SNR, pulsars
- Secondary source from spallation of primary CR nuclei
- DM annihilation/decay

Approaches

- Semi-analytical solution base on two-zone diffusion model.
- Fully numerical solution using real astrophysical data.
  GALPROP/Dragon code

Details on Processes Involved in CR Diffusion

See talks in AMS Days: I.V. Moskalenko, V.S. Ptuskin, K. Blum, S. Sarkar

Diffusion (magnetic field)

$$\hat{\mathcal{L}}_D\psi = \nabla(D_{xx}\nabla\psi)$$

$$D_{xx} = \beta D_0 \left(\frac{\rho}{\rho_0}\right)^{\delta_1,\delta_2}, \quad \beta = v/c$$

- Spatial diffusion coefficient D_{xx}
- Normalization constant D_0 could become a larger constant at higher energy
- Rigidity of CR particle $\rho = p/(Ze)$
- Below(above) a reference rigidity: δ_1 (δ_2)
- D_0 , δ_1(δ_2) determined via the ratio between secondary and primary cosmic-ray species: Boron to Carbon (B/C) Isotopes of Beryllium ^{10}Be/^{9} Be.

Convection (galactic wind)

$$\nabla V_c\psi(r,z) - \frac{\nabla V_c}{3}\frac{1}{p^2}\frac{\partial}{\partial p}(p^3\psi(r,z))$$

$$\left(\frac{dE}{dt}\right)_{\rm Adiab} = -E\left(\frac{2m+E}{m+E}\right)\frac{V_c}{2h}$$

Vc - along the z-direction perpendicular to the galactic disc.

Reacceleration para. (disturbances)

Relation between D_{pp} and D_{xx}

$$\frac{\partial}{\partial p}p^2 D_{pp}\frac{\partial}{\partial p}\frac{1}{p^2}\psi$$

$$D_{pp} = \frac{4V_a^2 p^2}{3D_{xx}\delta\left(4-\delta^2\right)\left(4-\delta\right)w},$$

Va - Alfven speed

Details on Processes Involved in CR Diffusion

Energy loss

For nuclei

- Ionization/Coulomb scattering

For electrons

- Inverse Compton scattering
- Synchrotron

Interstellar Medium (ISM) gas distribution

- simple parameterizations
- Using real data

ISM magnetic field

$$B_0 \exp\left(-\frac{R-R_\odot}{R_B}\right)\exp\left(-\frac{|z|}{z_B}\right),$$

$B_0 = 5\times10^{-10}$ Tesla, $R_B = 10$ kpc, $z_B = 2$ kpc

distance: sun to galactic center $r_\odot \approx 8.5$ kpc

Spallation/secondary generation

$$N_1 + (\mathrm{H},\mathrm{He}) \rightarrow N_2 + X$$

e.g.

^{11}C+H →^{11}B +X

Interstellar Flux of CRs

$$\Phi = \frac{v}{4\pi}\psi(\boldsymbol{r},p)$$

Solar modulation (force-field approximation)

Flux at top of the atmosphere of the Earth

$$\Phi^{\mathrm{TOA}}(T_{\mathrm{TOA}}) = \left(\frac{2mT_{\mathrm{TOA}}+T_{\mathrm{TOA}}^2}{2mT+T^2}\right)\Phi(T),$$

Kinetic energy of the cosmic-ray at TOP

$$T_{\mathrm{TOA}} = T - \phi_F \qquad \phi_F = 0.55\ \mathrm{GV}$$

Sources of CRs

- **Primary sources** (SNR)

Broken power low behavior in CR rigidity

$$\frac{dq_A(p)}{dp} \propto \left(\frac{\rho}{\rho_{As}}\right)^{\gamma_A}$$

Power law indices: γ_{p1} , γ_{p2} , γ_{e1} , γ_{e2} , γ_{e3}

Spatial distribution $q_A(R,z) =$

$$q_0 \left(\frac{R}{R_\odot}\right)^{\eta} \exp\left[-\xi \frac{R-R_\odot}{R_\odot} - \frac{|z|}{0.2\ \mathrm{kpc}}\right] ,$$

- q0 normalization parameter (fixed by EGRET gamma-ray data). $\eta = 0.5, \xi = 1.0$
- **Secondary sources (pp, pHe collision)**

$$q(p) = \beta c n_i \sum_{i=\mathrm{H,He}} \int dp' \frac{\sigma_i(p,p')}{dp'} n_p(p')$$

- **n** -number density of hydrogen, helium, and primary cosmic-ray proton per total momentum; differential cross section for

$$p + \mathrm{H(He)} \rightarrow \bar{p} + X$$

- **Primary sources of DM** (annihilation)

$$q(\boldsymbol{r}, p) = \frac{\rho(\boldsymbol{r})^2}{2m_\chi^2} \langle \sigma v \rangle \sum_X \eta_X \frac{dN^{(X)}}{dp},$$

$dN^{(X)}/dp$ injection spectra of annih. particle (for antiproton calculated by using numerical package PYTHIA)

- DM halo profiles: The energy density from N-body simulations

$$\rho(r) = \rho_\odot \left(\frac{r}{r_\odot}\right)^{-\gamma} \left(\frac{1+(r_\odot/r_s)^\alpha}{1+(r/r_\odot)^\alpha}\right)^{(\beta-\gamma)/\alpha}$$

$\rho_\odot \approx 0.43\ \mathrm{GeV\ cm^{-3}}$ local DM energy density

	α	β	γ	$r_s(\mathrm{kpc})$
NFW	1.0	3.0	1.0	20
Isothermal	2.0	2.0	0	3.5
Moore	1.5	3.0	1.5	28.0

Simplified Two-zone Diffusion Model

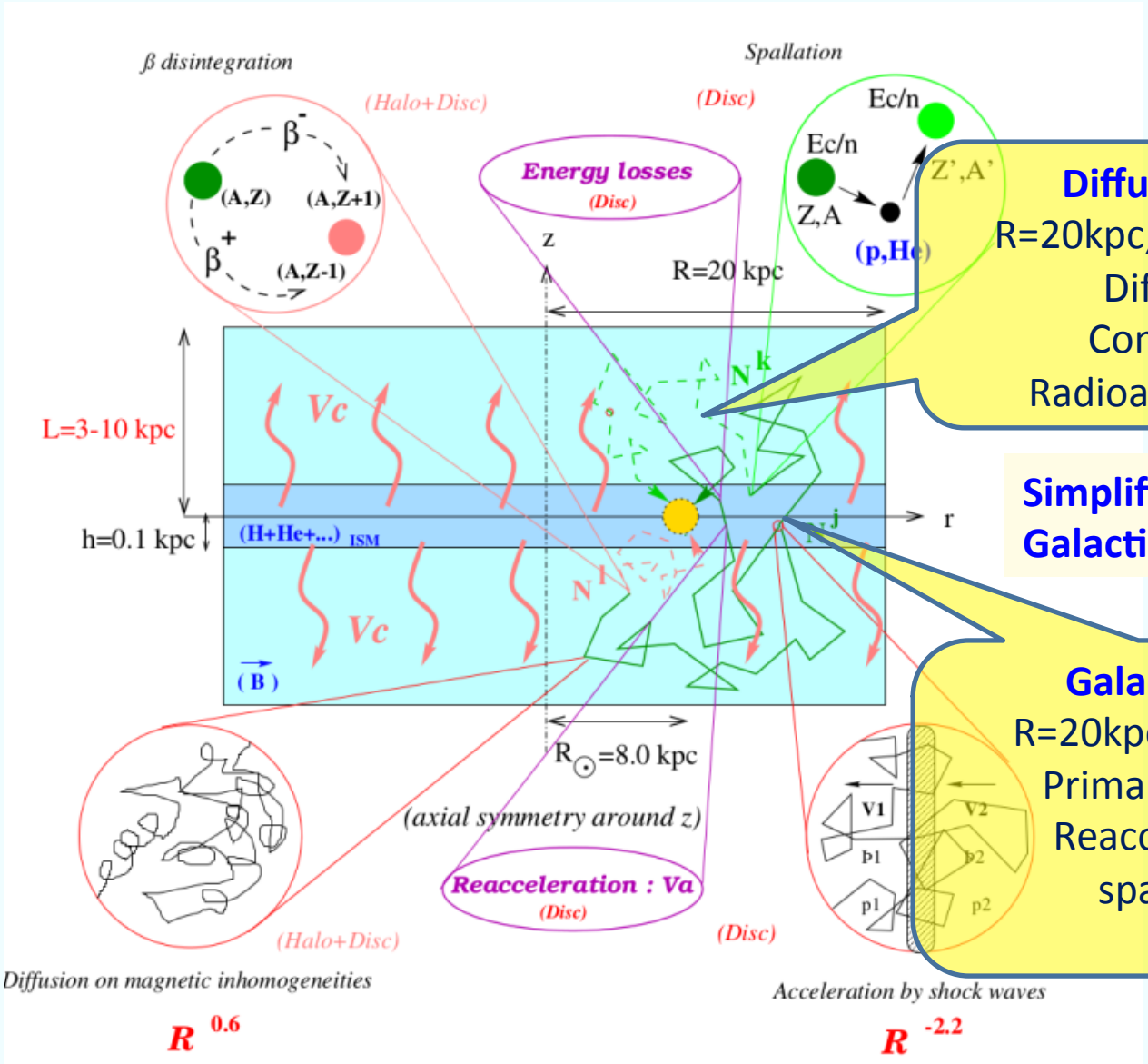

Diffusion halo
R=20kpc, Zh=1-10 kpc
Diffusion,
Convection
Radioactive decay

Simplified Assumptions on Galactic gas distribution

Galactic disk,
R=20kpc, h=0.1 kpc
Primary sources
Reacceleration
spallation

Maurin, etal, astro-ph/0212111

Approximate Solutions

For the source in the disk $q(r,z) = q(r)\delta(z)$ Hisano, hep-ph/0511118

Solution in Bessel expansion

$$\psi(r,z) = \exp\left(\frac{V_c z}{2K}\right) \sum_{i=0} \frac{Q_i}{A_i} \frac{\sinh[S_i(L-z)/2]}{\sinh[S_i L/2]} J_0(\zeta_i r_i/R)$$

with

$$A_i = 2h\Gamma_{inel} + V_c + K S_i \coth(S_i L/2)$$

$$S_i^2 = \frac{4\zeta^2}{R^2} + \frac{V_c^2}{K^2} + \frac{4\Gamma_{inel}}{K}$$

For DM sources (e.g. positrons) Maurin, astro-ph/0212111

Solution in Bessel and Fourier double expansion

$$\psi(r,z) = \sum_{n,m=1} A_{nm} J_0(\zeta_n r/R) \sin[m\pi(z-L)/2L]$$

$$A_{nm} = \int E' Q_{nm}(E') \frac{\tau}{E^2} \exp\left[\left(\frac{\zeta_n^2}{R} + \frac{m^2\pi^2}{4L^2}\right) K_0 \tau \left(\frac{E^{\delta-1}}{\delta-1} - \frac{E'^{\delta-1}}{\delta-1}\right)\right]$$

IMPLICATIONS OF AMS-02 RESULTS

with Unprecedented Accuracy (I)

DM Annihilation and Decays

Propagation Models

Two Benchmark Models

- Model A -Conventional model: Strong, Moskalenko, astro-ph/0101068, $\rho_e = 4$ GV $\rho_p = 9$ GV
- Model B -Constrained Model from global Byesian fit to B/C, $\rho_e = 4$ GV $\rho_p = 10$ GV

^{10}Be/^{9} Be, Carbon, Oxegen, etc. and Markov Chain Monte Carlo Trotta, etal, arXiv:1011.0037

Model	z_h(kpc)	D_0	δ_2	γ_{e1}/γ_{e2}	γ_{p1}/γ_{p2}
A	4.0	5.75	0.34	1.6/2.5	1.82/2.36
B	3.9	6.59	0.30	1.6/2.5	1.91/2.42

$\rho_0 = 4$ GV

$V_a = 36.0$ km s^{-1}

$V_a = 39.2$ km s^{-1}

Uncertainties and Correlations of propagation parameters In Model B

68% and 95% C.L. ; Best-fit value (red cross) , statistic mean value(green circle)

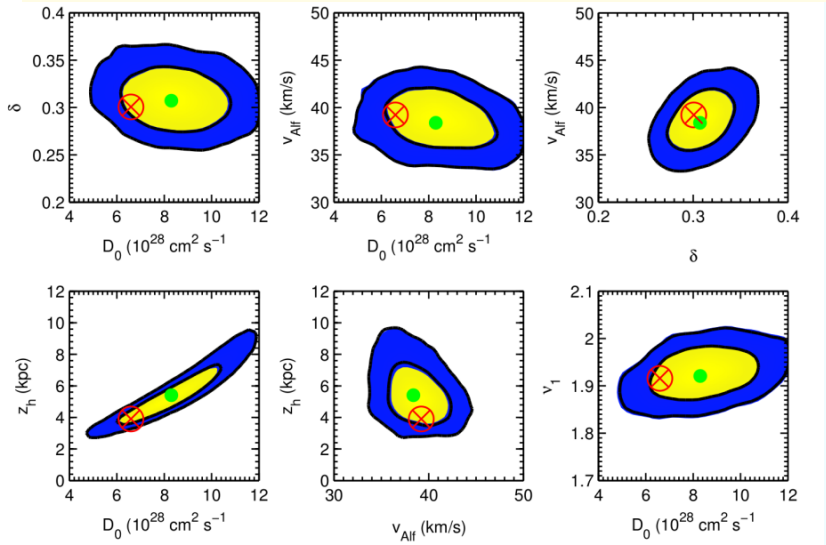

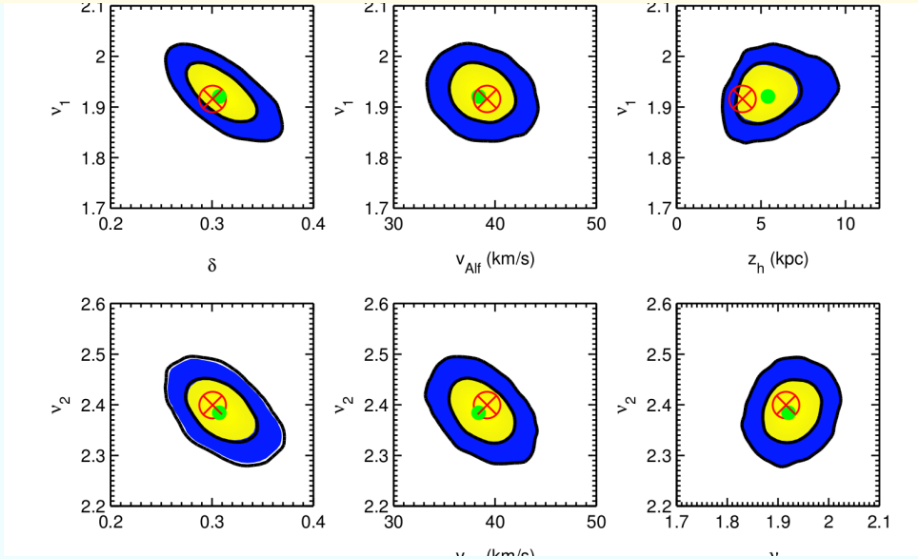

Propagation Models: extreme cases

Parameter range at 95%CL (Trotta, etal, arXiv:1011.0037)

$$Z_h = (3.2 - 8.6)\ \mathrm{kpc}, D_0 = (5.45 - 11.2) \times 10^{28}\ \mathrm{cm^2 s^{-1}}, \delta_2 = 0.26 - 0.35,$$

$$\gamma_{p1} = 1.84 - 2.00, \gamma_{p2} = 2.29 - 2.47, V_a = (34.2 - 42.7)\ \mathrm{km\ s^{-1}}.$$

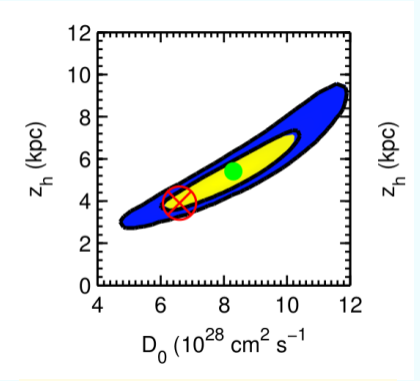

Z_h-D_0 correlation

We consider some extreme cases with params on the limits

- **C1(C2): Diffusion halo height Z_h and diffusion coefficient D_0**
- **D1(D2): Power index δ_2**
- **E1(E2) : Power index primary proton γ_{p2}**

Model	z_h(kpc)	D_0	δ_2	γ_{e1}/γ_{e2}	γ_{p1}/γ_{p2}
A	4.0	5.75	0.34	1.6/2.5	1.82/2.36
B	3.9	6.59	0.30	1.6/2.5	1.91/2.42
C1(C2)	3.2(8.6)	5.45(11.2)	0.30	1.6/2.5	1.91/2.42
D1(D2)	3.9	6.59	0.26(0.35)	1.6/2.5	1.91/2.42
E1(E2)	3.9	6.59	0.30	1.6/2.5	1.91/2.29(2.47)

Uncertainties in Primary Electrons

Instead of varying the power index primary electron γ_{e2} , the expressions for the total flux and positron fraction are modified to be

$$\Phi_{\rm tot} = \left(\kappa(E/{\rm GeV})^{\delta}\Phi_{e^-}^{\rm bg} + \Phi_{e^+}^{\rm bg}\right) + (\Phi_{e^-}^{\rm DM} + \Phi_{e^+}^{\rm DM}),$$

$$R_{e^+} = (\Phi_{e^+}^{\rm DM} + \Phi_{e^+}^{\rm bg})/\Phi_{\rm tot},$$

The normalization (κ) and slope (δ) of primary electron flux are set free.

At high energies $\Phi_{e^+}^{\rm bg} \ll \Phi_{e^+}^{\rm DM} \ll \Phi_{e^-}^{\rm bg}$

$$R_{e^+} \approx \frac{\Phi_{e^+}^{\rm DM}}{\kappa(E/{\rm GeV})^{\delta}\Phi_{e^-}^{\rm bg}}.$$

The cross section and k are nearly degenerate in positron fraction. Such a degeneracy can be removed by including the measurements of electron fluxes by PAMELA and AMS-02

Data Selection

- **Data included** (energy >20 GeV, to avoid solar modulation)
  - PAMELA positron fraction: 4 data points
  - Fermi-LAT positron fraction: 10 data points
  - AMS02 positron fraction: 31 data points
  - PAMELA electron: 18 data points
  - AMS02 electron: 35 data points
  - Fermi-LAT electron+positron: 28 data points
- **Energy resolution** of each exp. taken into account
  - PAMELA: 5%
  - Fermi-LAT: 6% at 7GeV, 15% at 1TeV
  - AMS02: 1.4% at 100 GeV and above

Results for DM Annihilation

Channel	m_χ(GeV)	$\langle\sigma v\rangle$	κ	$\delta(\times 10^{-2})$	$\chi^2_{\rm tot}$/d.o.f
$2e$	407.1	67.8	1.064	-6.43	450.56/119
	404.9	55.9	1.079	-7.72	403.40/119
2μ	570.0	244	0.997	-4.12	343.25/119
	793.8	387	1.136	-8.71	299.60/119
2τ	1534.3	1780	1.154	-7.62	219.67/119
	1860.1	2230	1.234	-10.4	210.78/119
4e	423.5	59.0	0.924	-2.25	415.21/119
	664.2	115	1.106	-8.22	355.25/119
4μ	1095.7	497	1.049	-5.32	290.18/119
	1409.7	690	1.158	-9.01	262.22/119
4τ	3068.4	3860	1.186	-8.26	205.72/119
	3794.3	4980	1.260	-10.9	199.29/119

←Model A
←Model B

- Model B fits the data better than Model A
- Quality of Fits: 2e, 4e highly inconsistent,
  2μ, 4μ improved, 2τ, 4τ acceptable

$\chi^2/\text{d.o.f} < 2$

H.B.Jin, Y.L. Wu, Y.F. Zhou, arXiv:1304.1997

$\chi\chi \rightarrow e^+e^-$, Spectra too Sharp for All Models

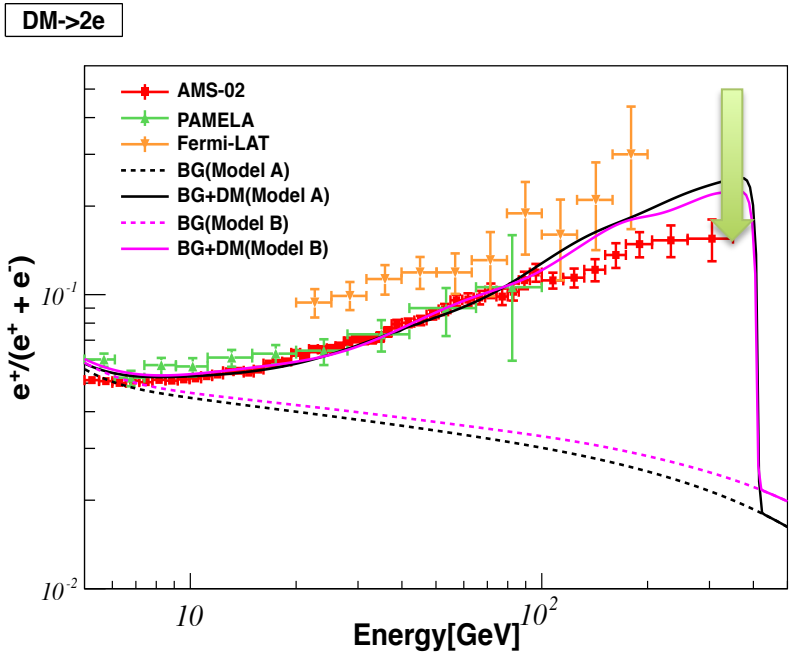

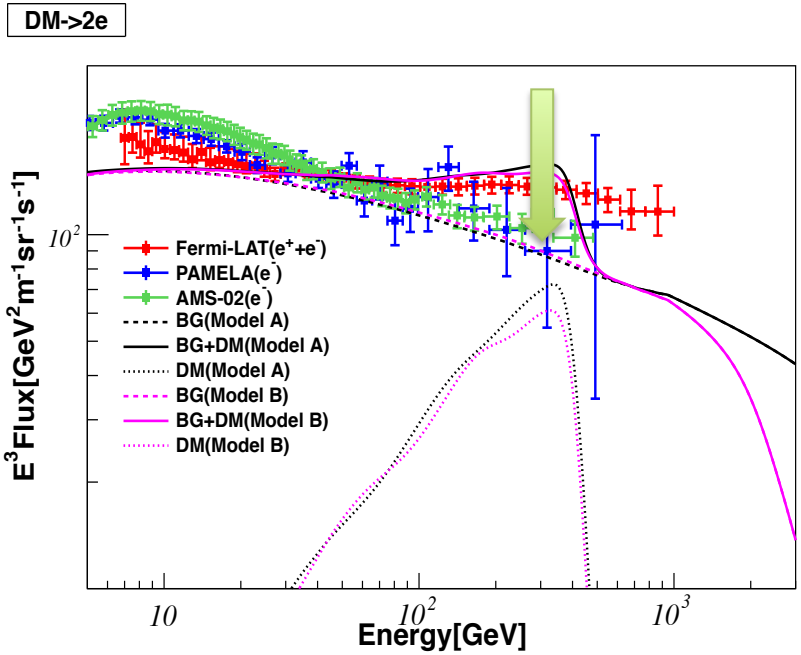

2e and 4e channels are inconsistent with both AMS02 and Fermi-LAT

H.B.Jin, Y.L. Wu, Y.F. Zhou, arXiv:1304.1997

Results: $\chi\chi \rightarrow \mu^+\mu^-$ for Benchmark Models

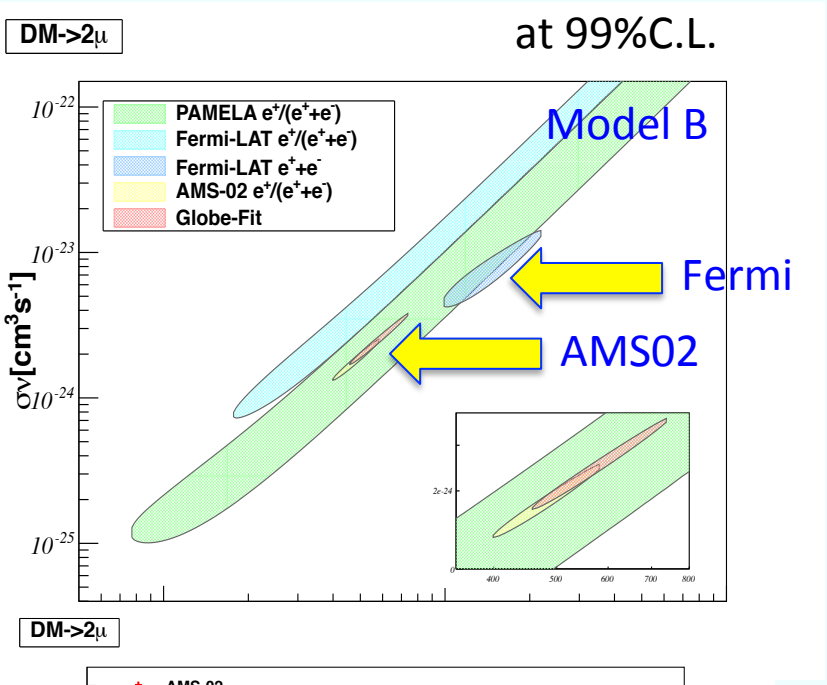

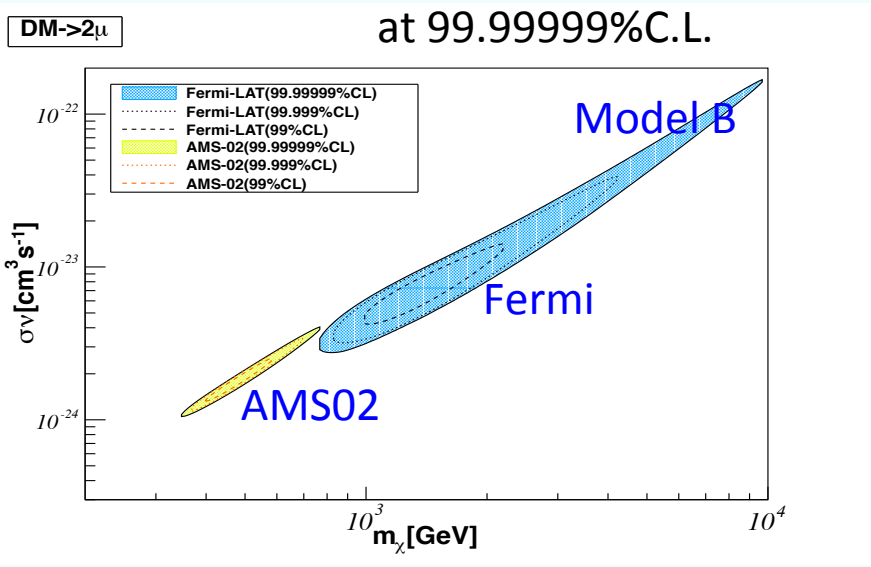

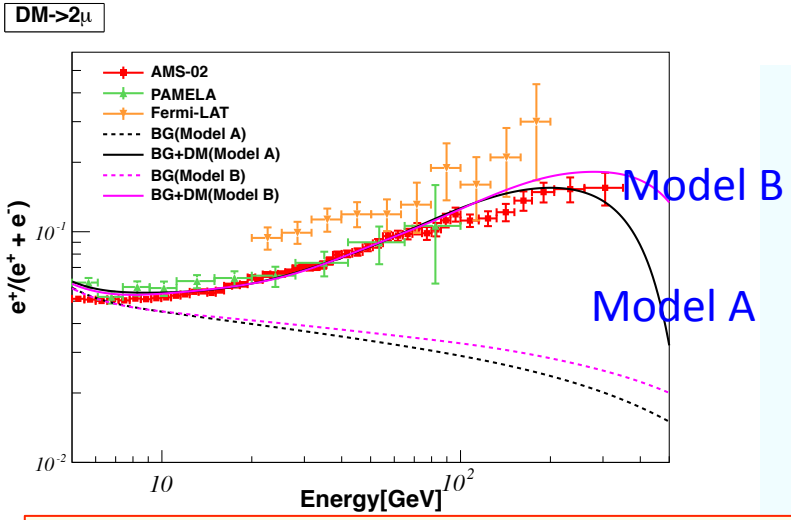

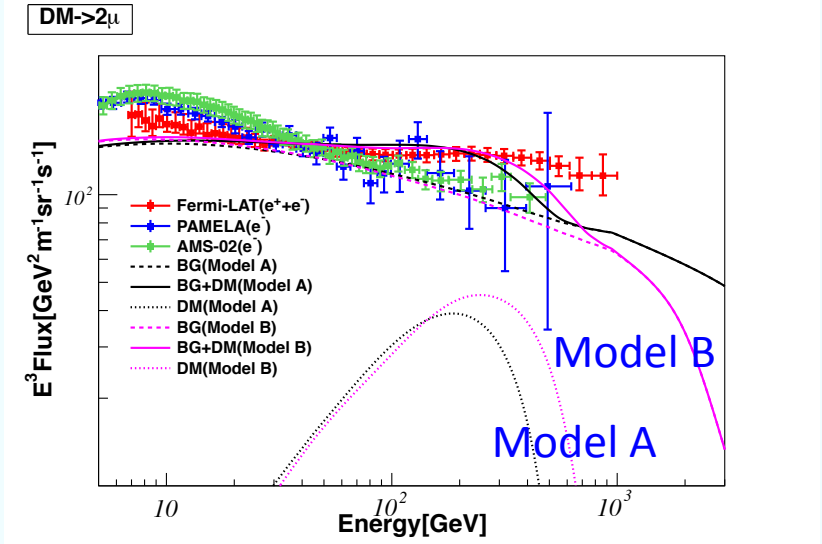

- 2μ channel is much improved and can fits both PAMELA and Fermi data
- Fermi-LAT data are inconsistent with the AMS02 data for 2μ channel

Results: $\chi\chi \rightarrow \mu^+\mu^-\mu^+\mu^-$

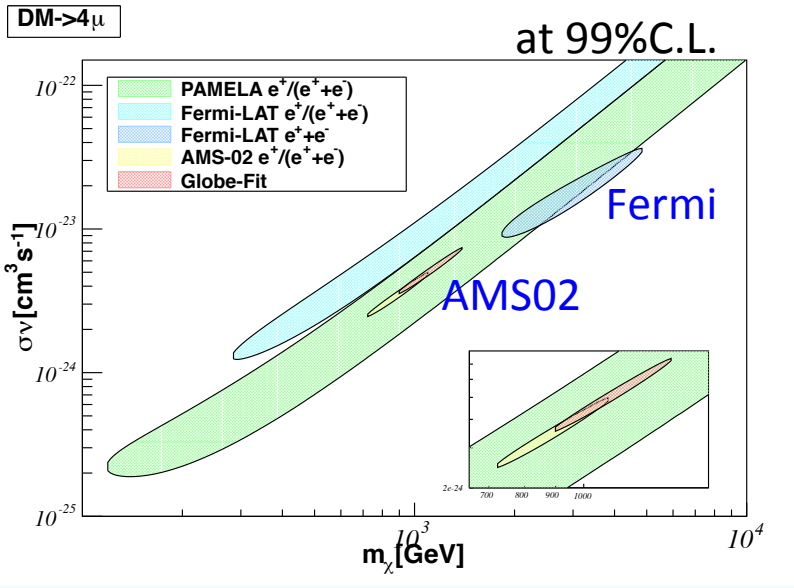

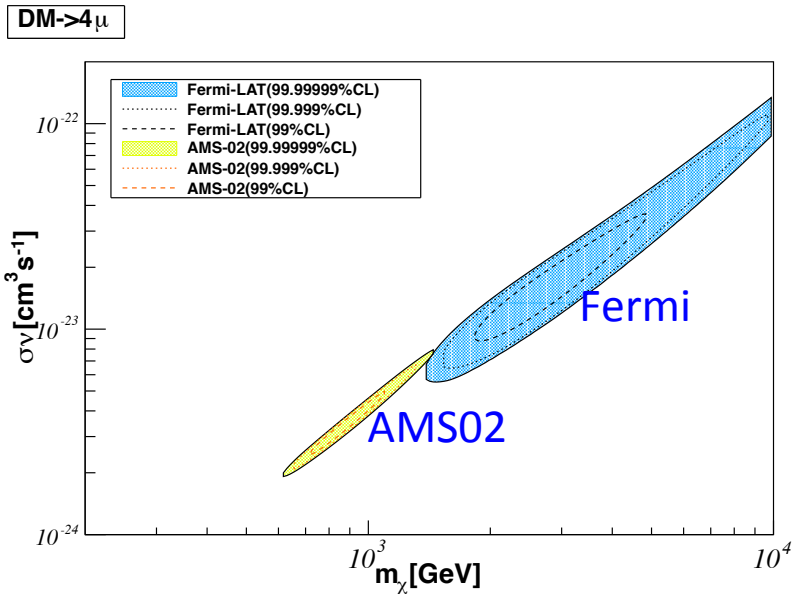

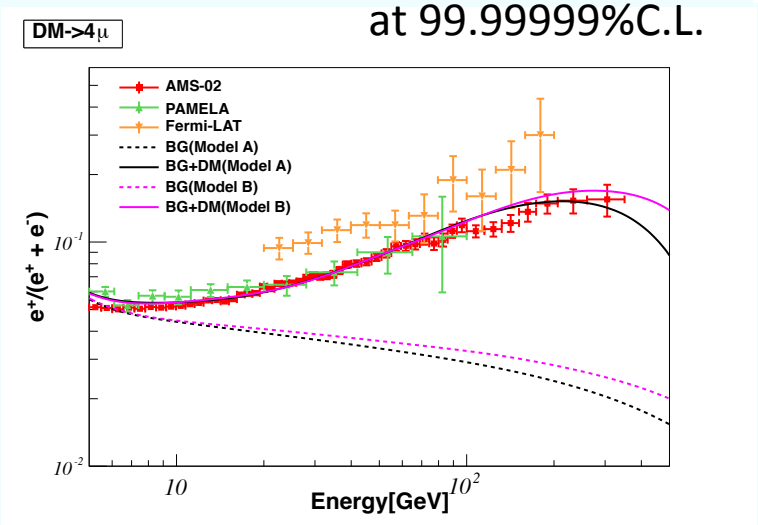

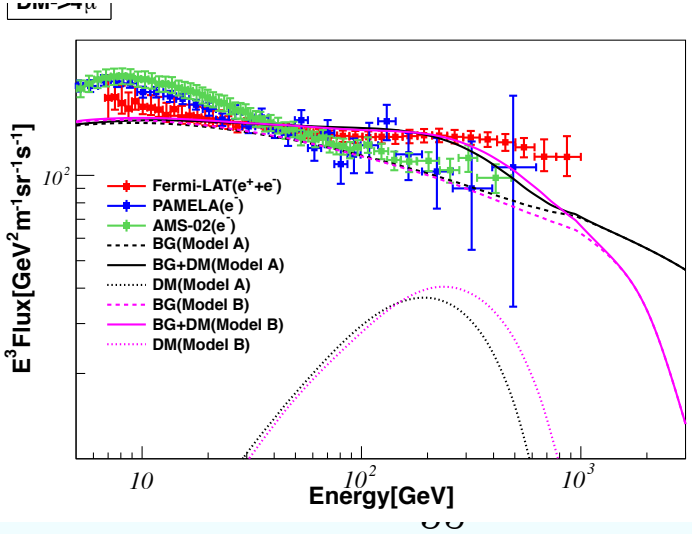

H.B.Jin, Y.L. Wu, Y.F. Zhou, arXiv:1304.1997

Results: $\chi\chi \rightarrow \mu^+\mu^-$, $\mu^+\mu^-\mu^+\mu^-$

Model C1,C2 with different (Z_h , D_0)

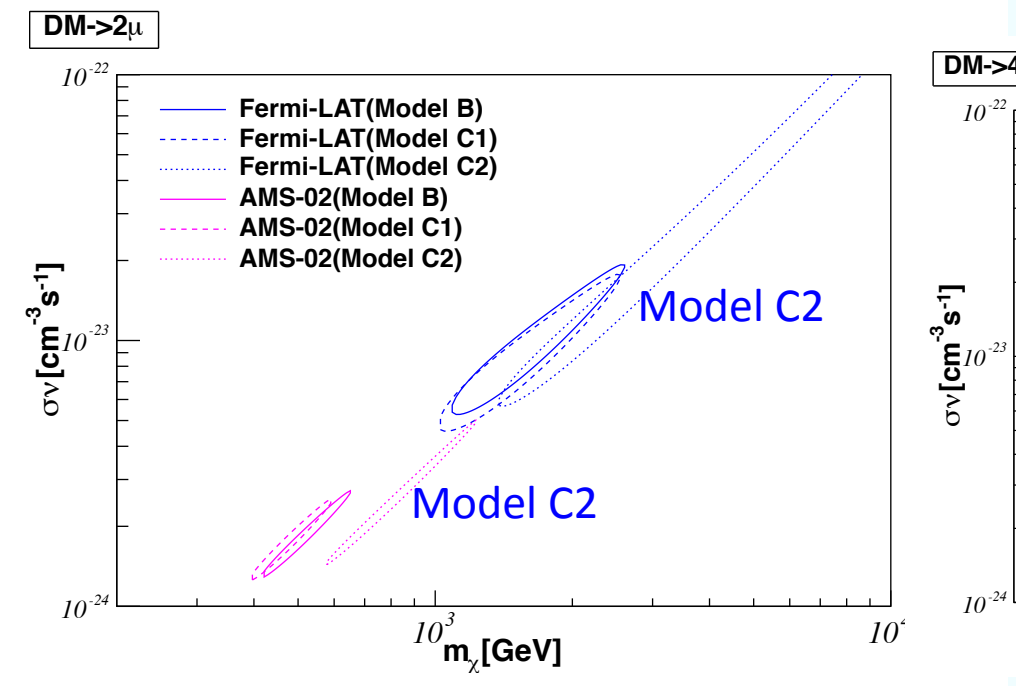

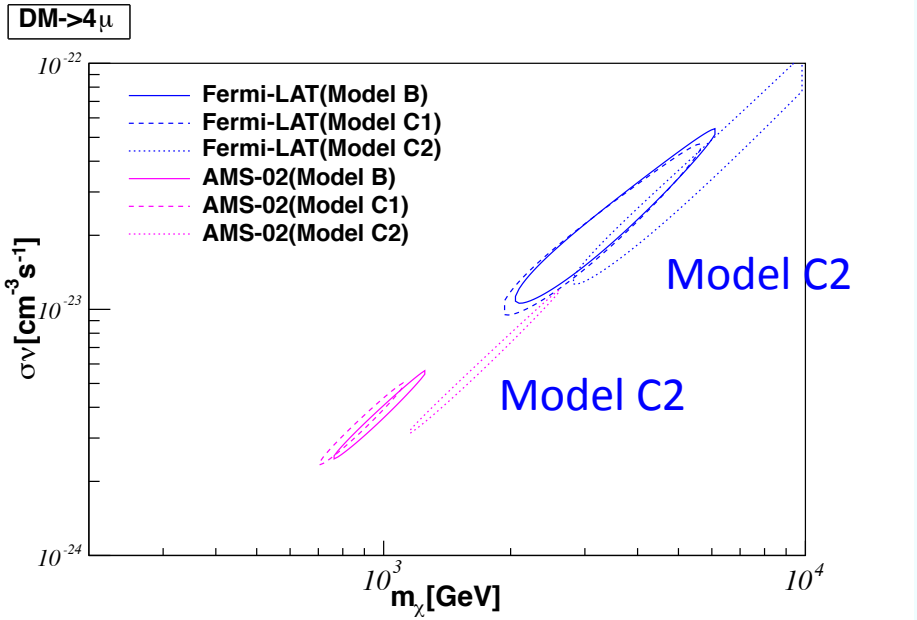

Tension between AMS02 and Fermi-LAT slightly reduced with large diffusion halo height Z_h=8.6 kpc and D_0=11.2

Results: $\chi\chi \rightarrow \mu^+\mu^-$, $\mu^+\mu^-\mu^+\mu^-$

model D1,D2 with different δ_2 , models E1,E2 with different γ_{p2}

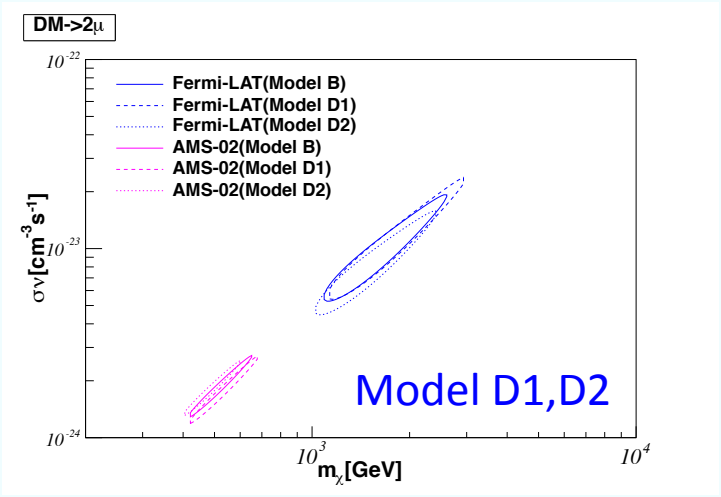

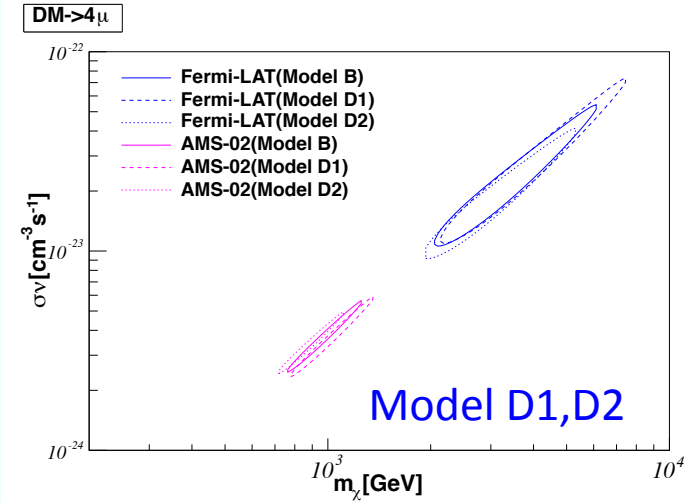

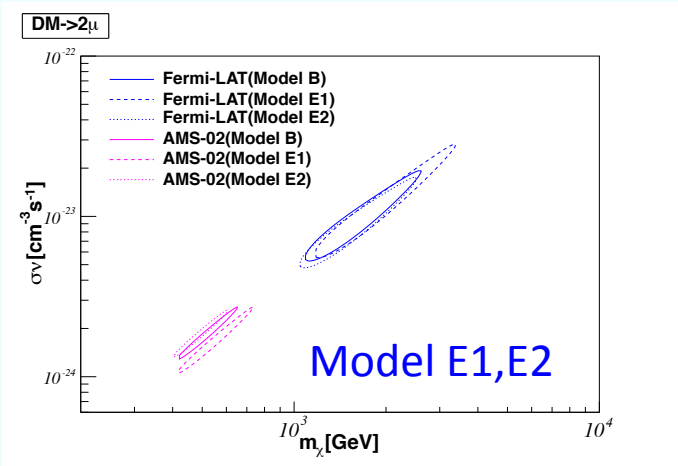

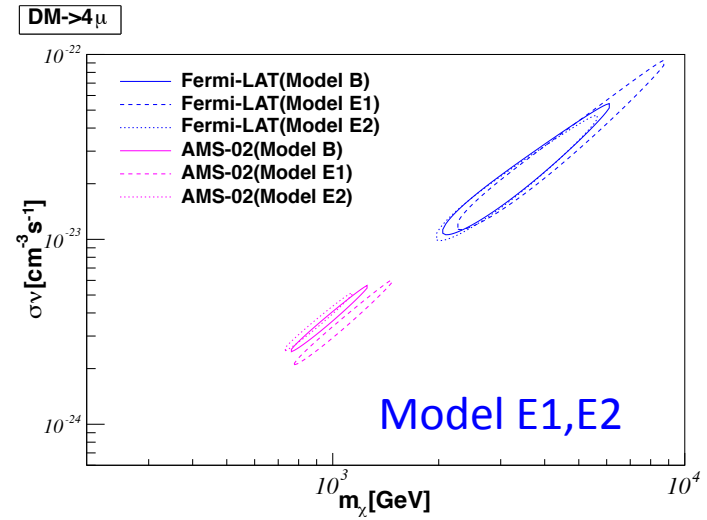

The tension between AMS02 and Fermi-LAT remains in models D1,D2,E1,E2

Results: $\chi\chi \rightarrow \tau^+\tau^-$

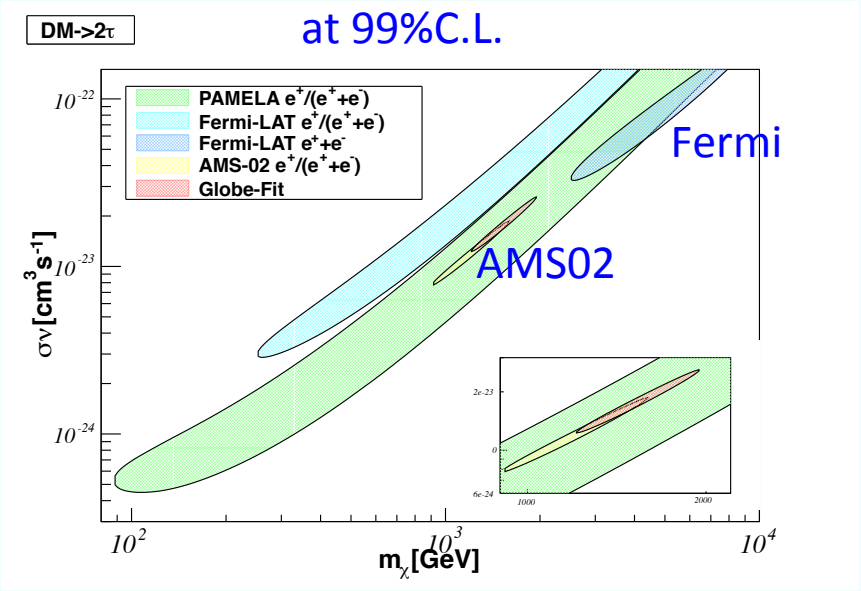

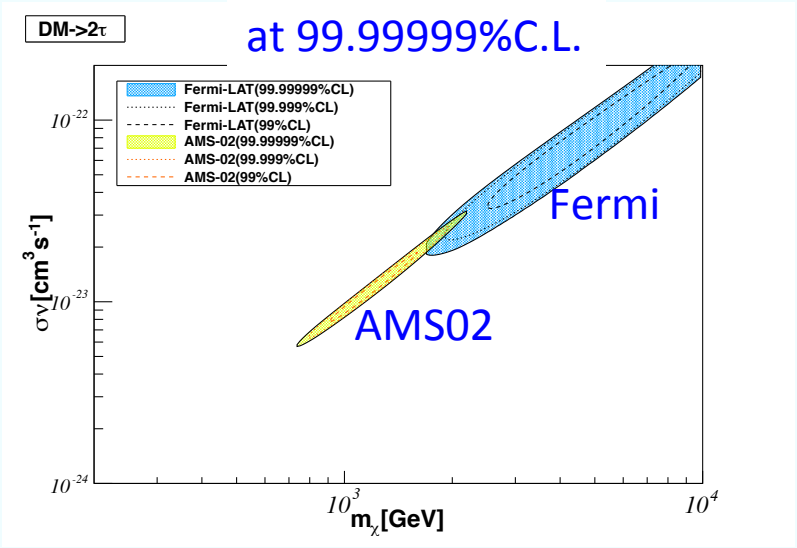

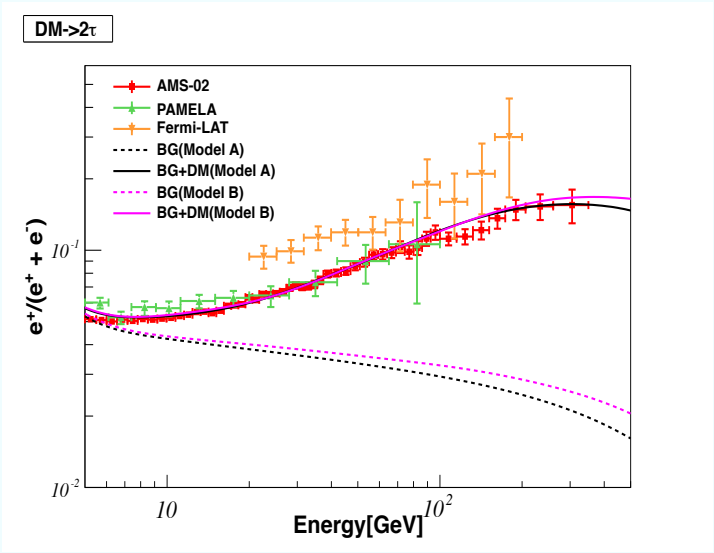

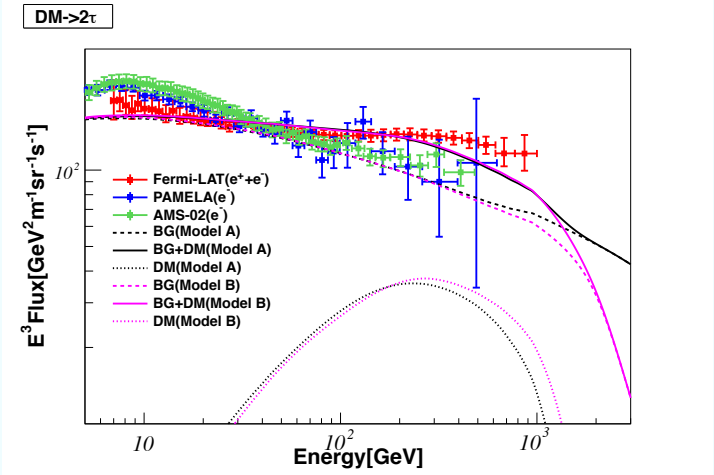

Fits slightly improved for 2τ, 4τ

DM Decay: $\chi\chi \rightarrow \tau^+\tau^-\tau^+\tau^-$

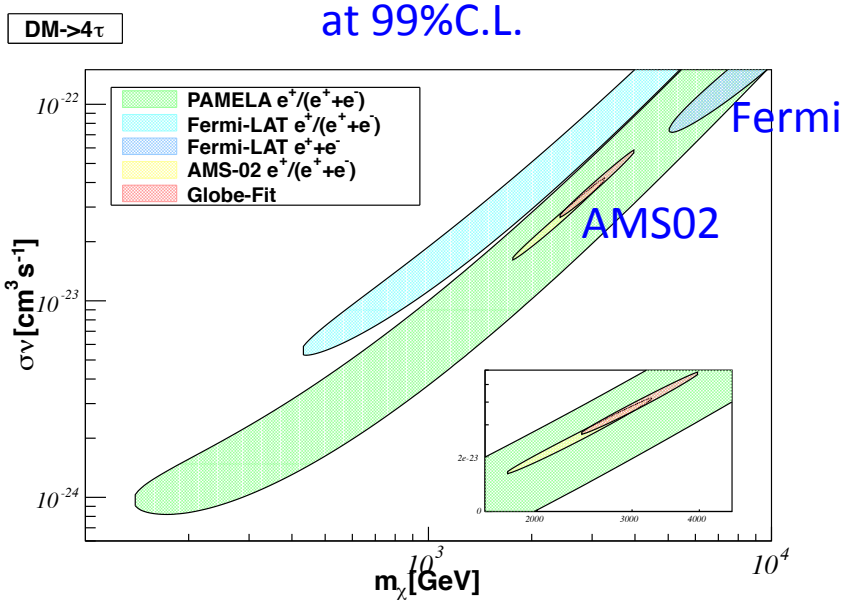

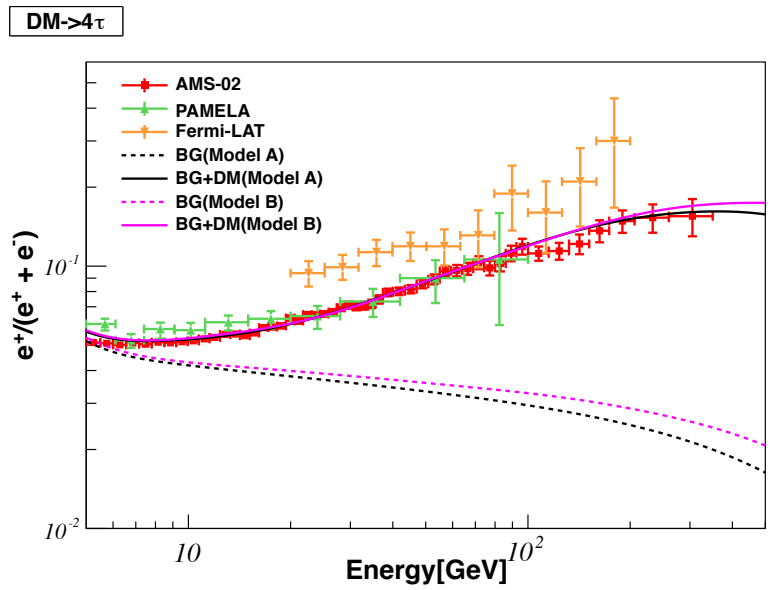

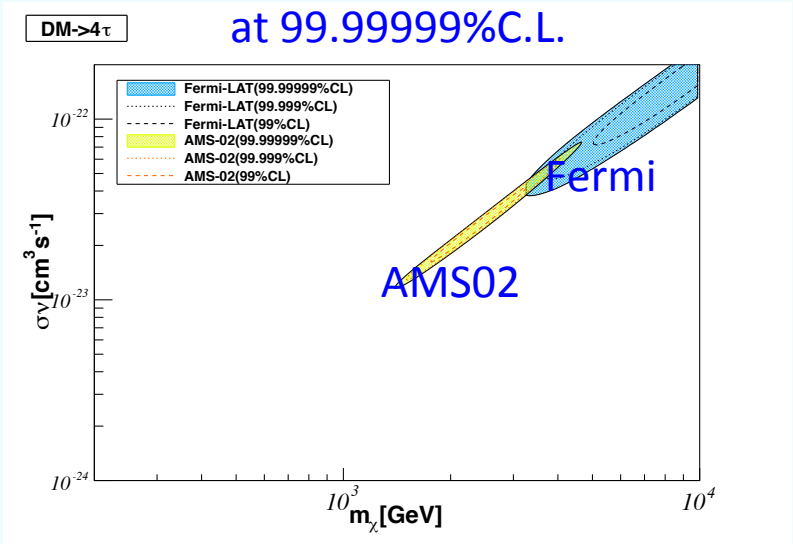

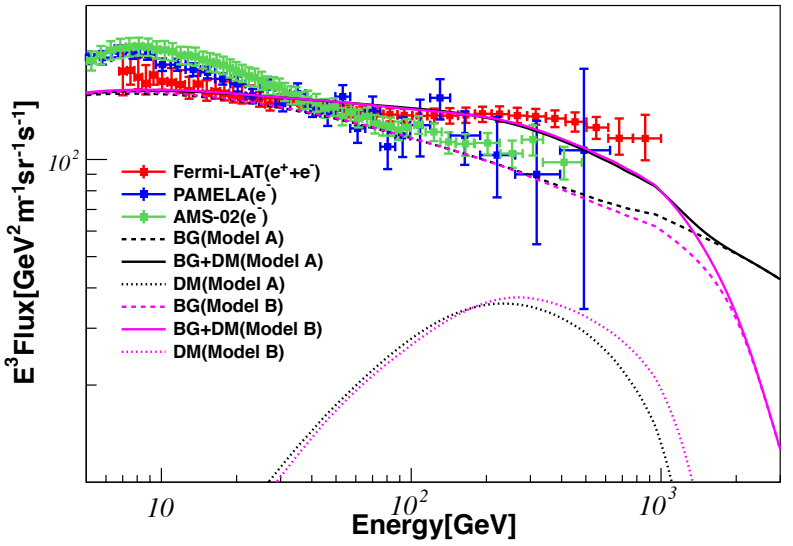

Results for DM Decay

mode	m_χ(GeV)	$\tau(\times 10^{26}\mathrm{s})$	κ	$\delta(\times 10^{-2})$	$\chi^2_{\mathrm{tot}}/\mathrm{dof}$	
$2e$	334.0	21.1	0.632	6.79	892.87/119	←Model A
	332.1	24.2	0.673	4.25	836.39/119	←Model B
2μ	654.8	6.27	0.806	1.40	510.77/119	
	691.1	6.39	0.856	-1.24	493.92/119	
2τ	1762.4	2.15	1.019	-4.41	291.92/119	
	1860.1	2.19	1.072	-6.79	291.56/119	
$4e$	506.2	19.3	0.737	3.54	622.69/119	
	523.7	19.9	0.787	0.81	594.44/119	
4μ	1258.6	5.76	0.882	-0.78	414.90/119	
	1328.4	5.85	0.933	-3.32	406.53/119	
4τ	3455.5	1.97	1.058	-5.34	265.93/119	
	3647.0	2.01	1.112	-7.69	266.56/119	

Quality of Fits: DM decay is not as good as DM annihilation

H.B.Jin, Y.L. Wu, Y.F. Zhou, arXiv:1304.1997

Allowed Regions from DM Decay

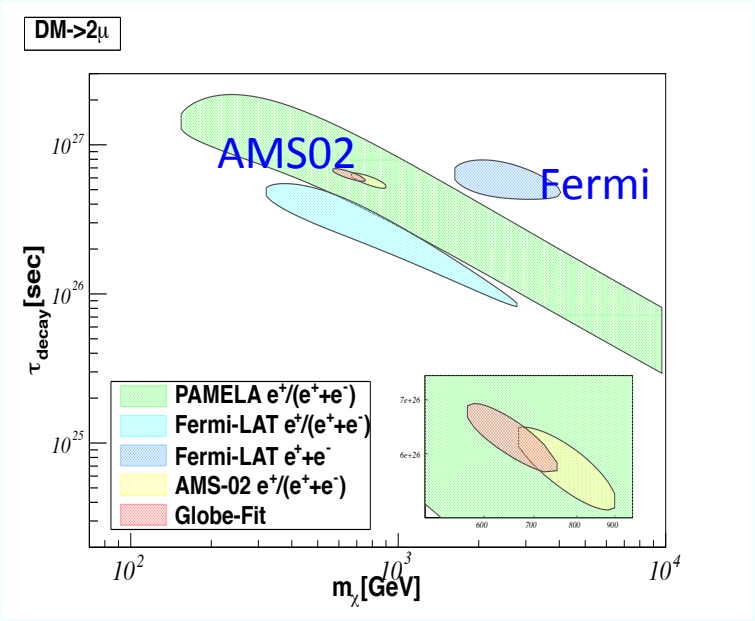

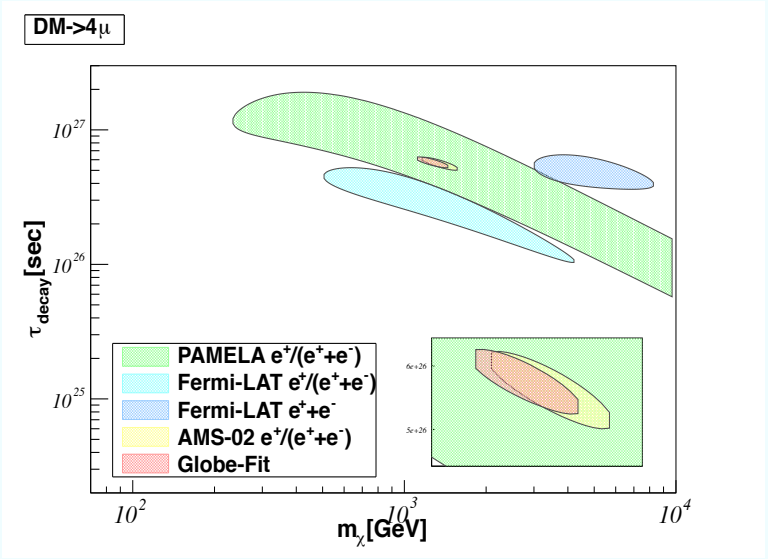

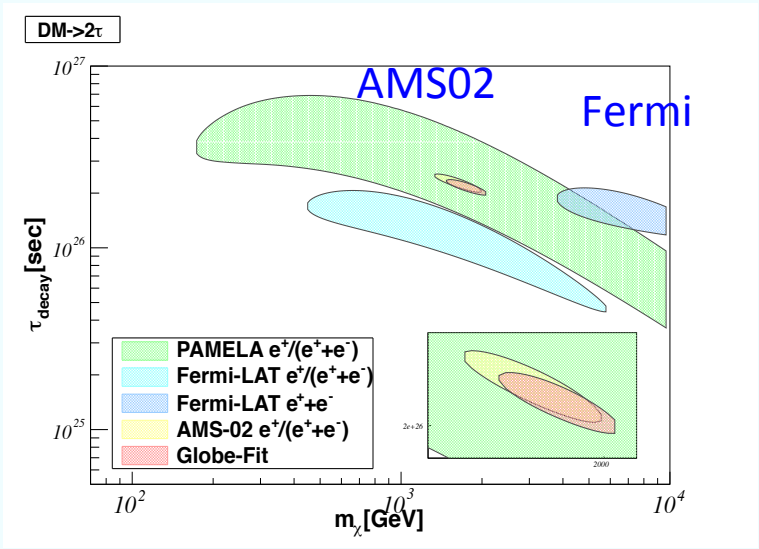

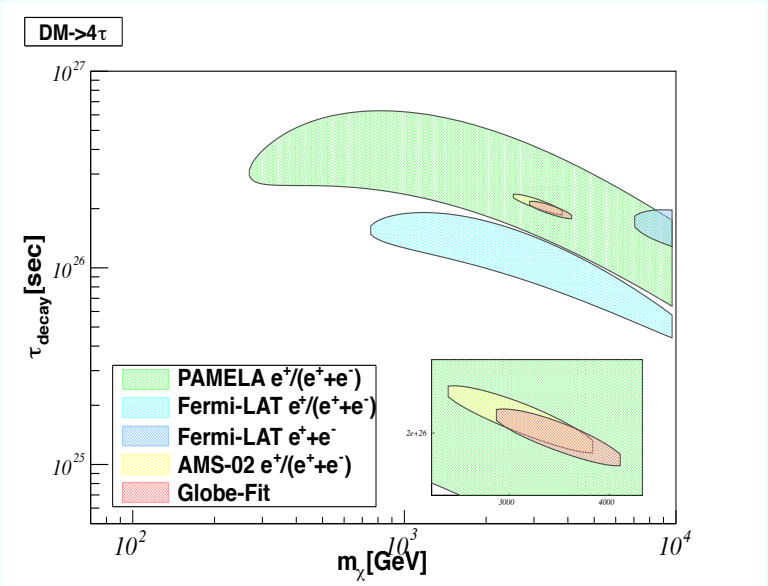

DM Asymmetric Decay

for $\chi \neq \bar{\chi}$, $\rho(r) \neq \bar{\rho}(r)$

$$\rho(\mathbf{r}) \equiv \rho_\chi(\mathbf{r}) + \rho_{\bar{\chi}}(\mathbf{r}),$$
$$\epsilon \equiv (\rho_\chi(\mathbf{r}) - \rho_{\bar{\chi}}(\mathbf{r}))/(\rho_\chi(\mathbf{r}) + \rho_{\bar{\chi}}(\mathbf{r})),$$

Source term

$$q_{e^\pm}(\mathbf{r}, p) = \frac{\rho(\mathbf{r})}{2\tau m_\chi}(1 \pm \epsilon) \sum_X \eta_X \frac{dN_e^{(X)}}{dp},$$

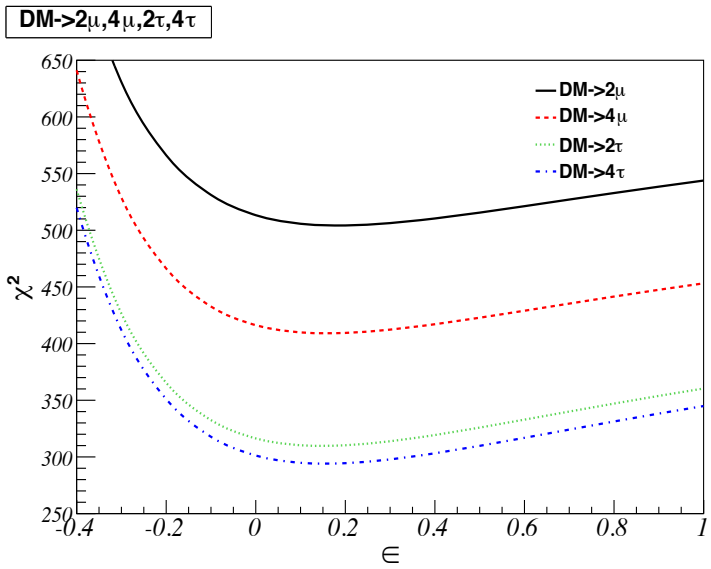

For fixed background κ=0.85, δ=0
No indication of non-zero ε ,
Symmetric Decay is favored

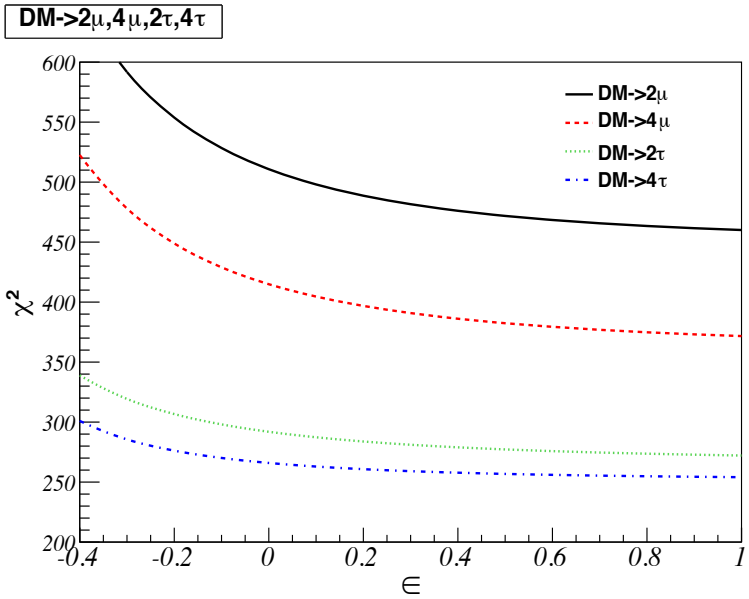

For varying backgrounds, ε=1 maximal asymmetric decay is slightly favored

IMPLICATIONS OF AMS-02 RESULTS

with Unprecedented Accuracy (II)

Can we make more stringent constraints on the CR propagation model from AMS-02 data?

How the backgrounds and DM signals may change in reference DM models

Constraining Propagation Models From CR Data

Observables

-- Secondary/Primary

- B/C and sub-Fe(Sc+V+Ti)/Fe

  sensitive to combination D_0/Z_h

-- Radioactive species

- $^{10}Be/^{9}Be$, $^{36}Cl/Cl$, $^{26}Al/^{27}Al$

  sensitive to diffusive halo size Z_h

-- Stable primaries

- Proton and Helium fluxes

  sensitive to primary sources

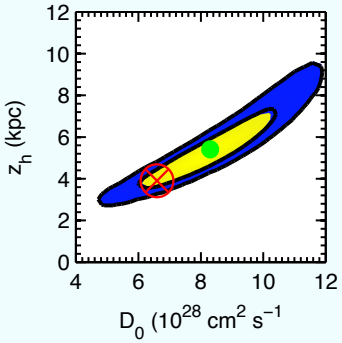

Trotta, etal, arXiv:1011.0037

Degeneracies in parameters

- D_0 and Z_h are almost degenerate
- V_a scales as $(D_0)^{1/2}$
- $\delta + \gamma_{p1}$ close to 2.72

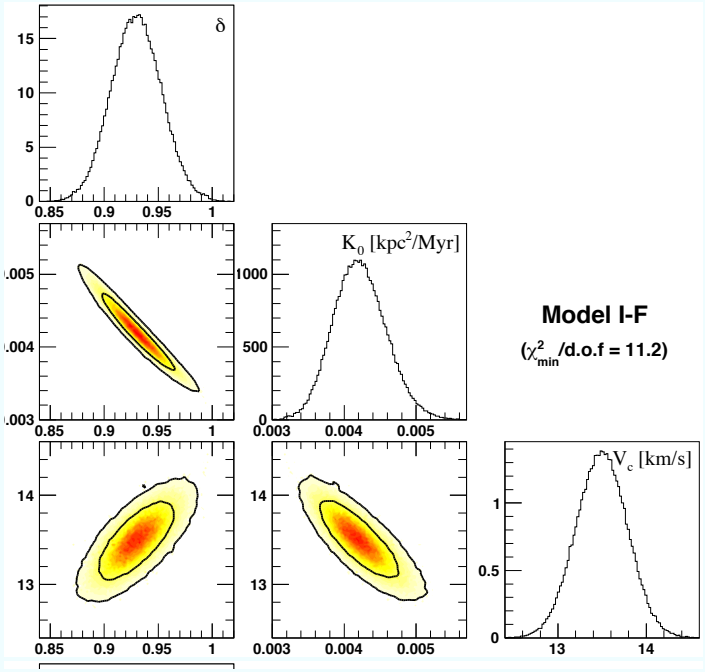

Maurin, etal, astro-ph/0212111

Analysis Using AMS-02 Data Alone

Previous analyses relay on combinations of B/C, isotopes ^{10}Be/^{9}Be, etc. which are measured from different experiments

Our Motivations:

1. AMS-02 is measuring the CRs with unprecedented accuracies
2. Avoiding combination of syst. errors in different experiments
3. All data from the same period, easy to model solar modulation effects
4. It is possible to determine the major parameters from AMS-02

$$\boldsymbol{\theta} = \{Z_h, D_0, \delta, V_a, \gamma_{p1}, \gamma_{p2}\}.$$

Using data Set: B/C ratio + Proton flux $D = \{D_{B/C}^{\rm AMS}, D_p^{\rm AMS}\}.$

proton flux is not just a power low in energy

(break at 10 GeV imposes constraints on V_a) $\rho_{ps} = 10^4$ MV

B/C → D_0/Z_h, V_a, δ (18 data points)

Proton → γ_1, γ_2, V_a (100 data points)

Proton flux spectrum constrains V_a , breaks V_a-- D_0 degeneracy, and enables the determination of Z_h

Normalization: at E =100GeV fit to AMS02 proton flux $N_p = 4.83 \pm 0.02$ cm^{-2}sr^{-1}s^{-1}MeV^{-1}

Breaking D_0/Z_h Degeneracy

Relative change with Z_h for fixed D_0/Z_h (E=20GeV)

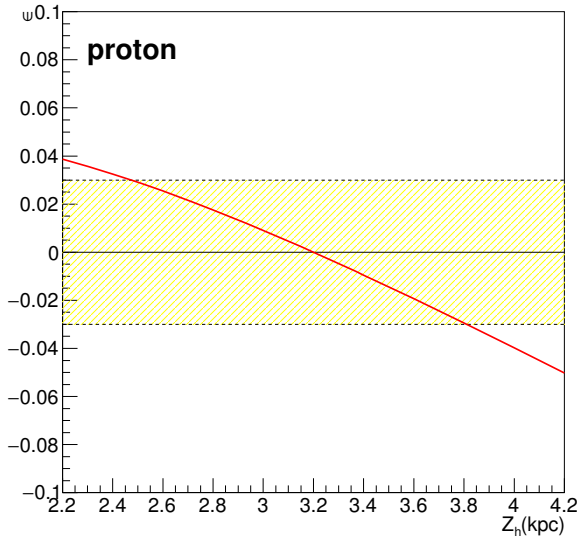

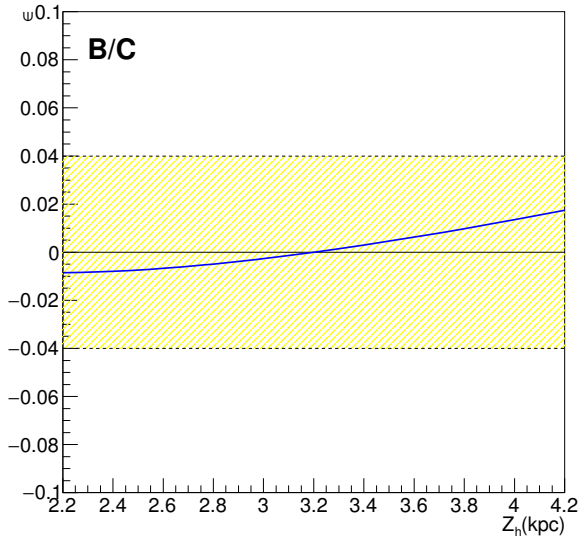

Conclusion: the spectrum of the primary cosmic-ray flux such as that of proton can impose constraints on both the propagation parameters and the primary sources.

Analytic solution in two-zone model

$$\psi_i(0) = \frac{2hq_i}{V_c + 2h/\tau_f + D_{xx}S_i \coth(S_i Z_h/2)},$$

$$S_i^2 = \frac{V_c^2}{D_{xx}^2} + \frac{4}{D_{xx}\tau_r} + \frac{4\zeta_i^2}{R_h^2}.$$

$$D_{xx}S_i \coth(S_i Z_h/2) \approx \left(\frac{D_{xx}}{Z_h}\right)\left(2 + \frac{V_c^2 Z_h^2}{6D_{xx}^2} + \frac{2Z_h^2}{3D_{xx}\tau_r} + \frac{2Z_h^2}{3R_h^2}\zeta_i^2\right).$$

D_0/Z_h degeneracy is slightly broken in stable CR fluxes

- For proton ~5%, data err ~3%
- For B/C ~2%, data error ~4%

Consequence

- B/C determines D_0/Z_h
- Proton determines Z_h

Method: Bayesian Inference

Posterior Probability Distribution Functions (PDF)

- Bayes's Theorem (posterior PDF)

$$p(\theta|D) = \frac{\mathcal{L}(D|\theta)\pi(\theta)}{p(D)}$$

- Bayesian evidence (quality of fit)

$$p(D) = \int_V \mathcal{L}(D|\theta)\pi(\theta)d\theta.$$

By Integrating over the whole volume of parameter space

- Marginal PDFs of interesting parameters

$$p(\theta_1, \ldots, \theta_n)_{\rm marg} = \int p(\theta|D) \prod_{i=n+1}^{m} d\theta_i$$

By Integrating out nuisance parameters

- Priors PDF (uniform-Flat distribution)

$$\pi(\theta_i) \propto \begin{cases} 1, & \text{for } \theta_{i,\min} < \theta_i < \theta_{i,\max} \\ 0, & \text{otherwise} \end{cases}$$

Likelihood function (Gaussian)

$$\mathcal{L}(D|\boldsymbol{\theta}) = \prod_i \frac{1}{\sqrt{2\pi\sigma_i^2}} \exp\left(-\frac{(f_{\rm th}(\theta) - f_{{\rm obs},i})^2}{2\sigma_i^2}\right)$$

Numerical methods

- MCMC sampling
- Metropolis-Hasting (algorithm) MCMC
- CosmoMC package

Statistic mean value

$$\langle\theta_i\rangle = \int \theta_i P(\theta_i|D)d\theta_i = \frac{1}{N}\sum_{k=1}^{N} \theta_i^{(k)}$$

Results

with 2.6x10^4 Markov Chain Monte Carlo (MCMC) samples

$R = 20$ kpc $\quad \delta_1 = \delta_2 \equiv \delta,$

$\Delta R = 1$ kpc $\quad \Delta Z = 0.2$ kpc

Quantity	Prior range	Best-fit value	Posterior mean and Standard deviation	Posterior 95% range	Ref. [23]
Z_h(kpc)	[1, 11]	3.2	3.3±0.6	[2.1, 4.6]	5.4±1.4
D_0/Z_h	[1, 3]	2.02	2.00±0.07	[1.82, 2.18]	(1.54±0.48)
δ	[0.1, 0.6]	0.29	0.29±0.01	[0.27, 0.32]	0.31±0.02
$V_a(\mathrm{km \cdot s^{-1}})$	[20, 70]	44.7	44.6±1.2	[41.3, 47.5]	38.4±2.1
γ_{p1}	[1.5, 2.1]	1.79	1.78±0.01	[1.75, 1.81]	1.92±0.04
γ_{p2}	[2.2,2.6]	2.46	2.45±0.01	[2.43,2.47]	2.38±0.04

D_0/Z_h is precisely determined (err <5% vs. 30%)

$$\frac{D_0}{Z_h} = (2.00 \pm 0.07)\ \mathrm{cm^2 s^{-1} kpc^{-1}}.$$

The fitting strategy is quite different, uncertainties in the parameters are significantly smaller !
uncertainty is within 5%

Z_h is determined with err up to ~ 20% (relative smaller 26%)

$Z_h = 3.3 \pm 0.6\mathrm{kpc}$ **40% lower (~5.4)**

$\chi^2/\mathrm{dof} = 49.0/112$

Trotta, 1011.0037 fit B/C + ^{10}Be/^{9}Be

B/C ratio from HEAO-3, ATIC-2 and CREAM-1, the data of ^{10}Be/^{9}Be from ACE , and the data of Carbon and Oxygen nuclei fluxes from ACE

1D Posterior Probability Distribution Functions (PDFs)

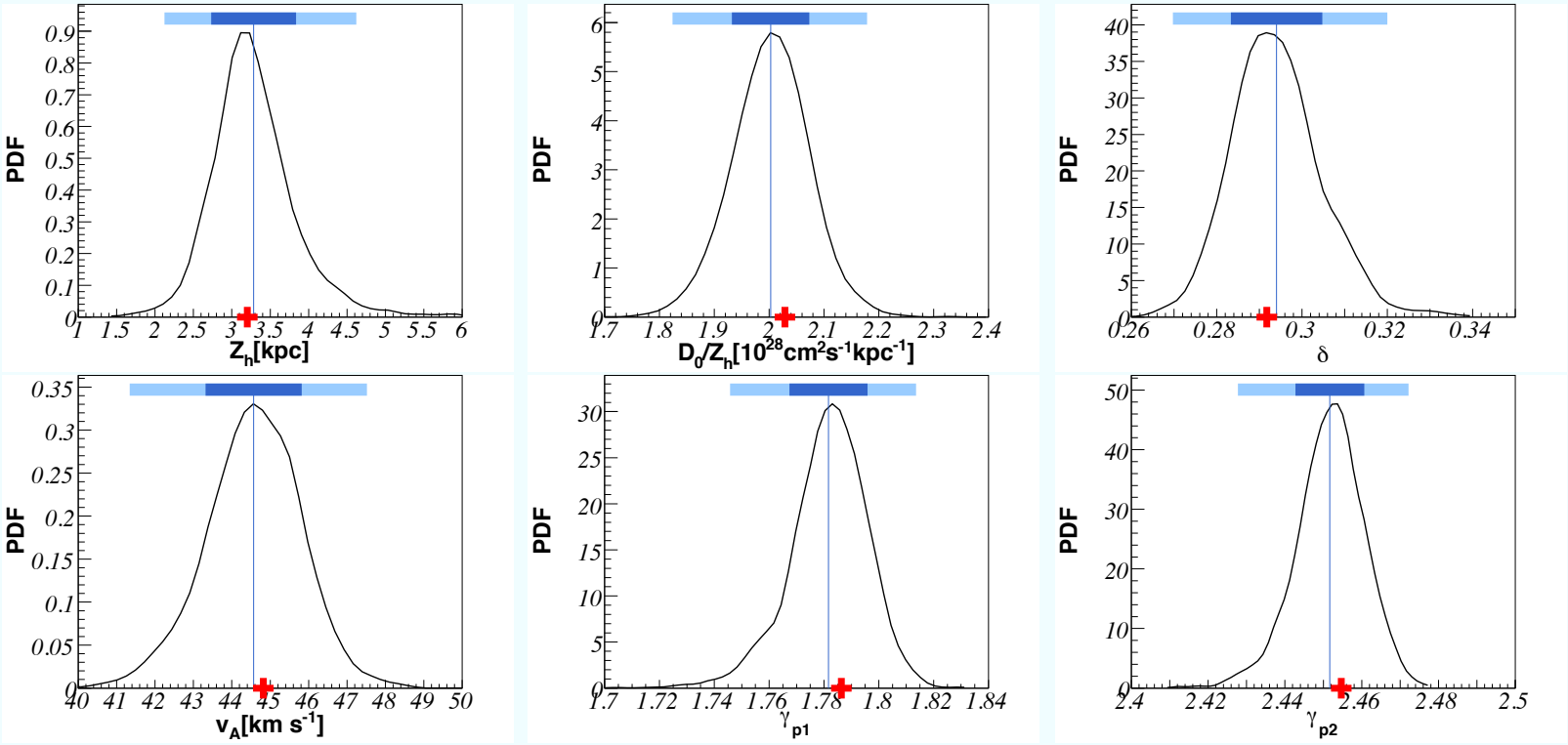

All the one-dimensional PDFs are close to Gaussian

$$p(\theta|D) = \frac{\mathcal{L}(D|\theta)\pi(\theta)}{p(D)}$$

Horizontal bar indicates the 1σ- and 2σ-standard deviations

Best-fit value (red plus), Statistic mean value (vertical line)

Two-dimensional Marginalized Posterior PDFs

68% C.L. -dark blue, 95% C.L. – blue;

Rest-fit value (red plus) , Statistic mean value(yellow cross)

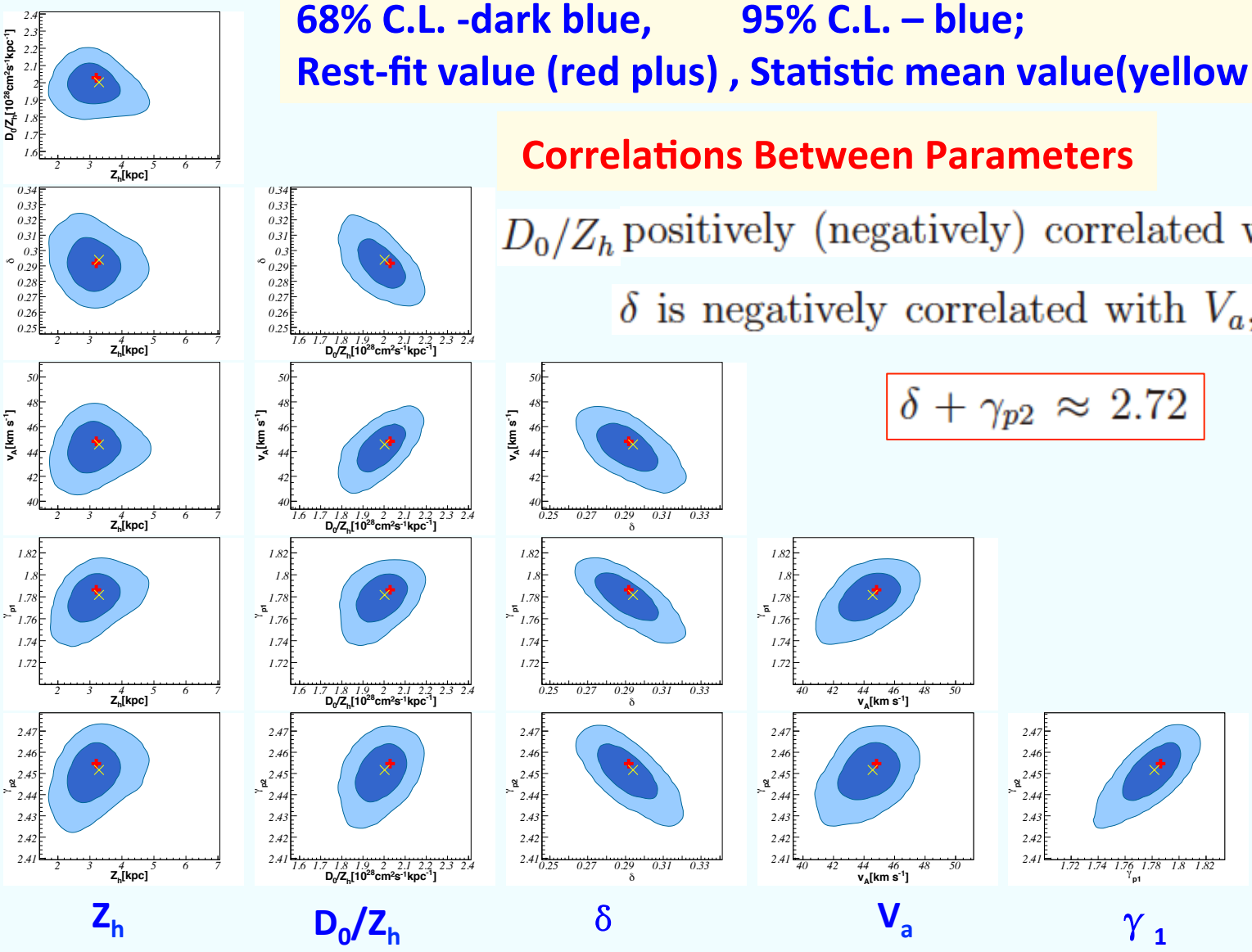

Correlations Between Parameters

D_0/Z_h positively (negatively) correlated with $V_a(\delta)$

δ is negatively correlated with V_a, $\gamma_{p1,p2}$

$$\delta + \gamma_{p2} \approx 2.72$$

Best-fits & Predictions for Backgrounds

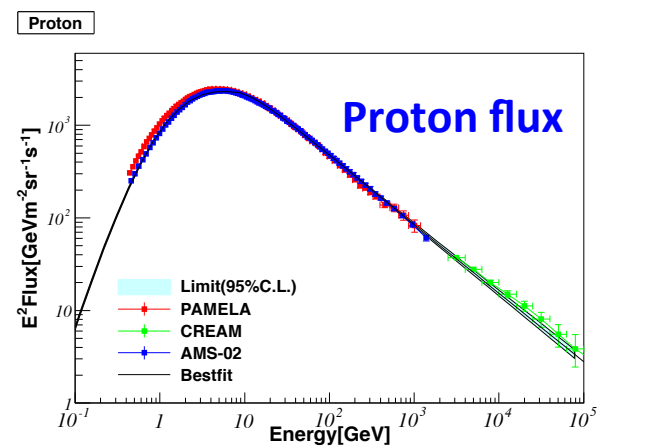

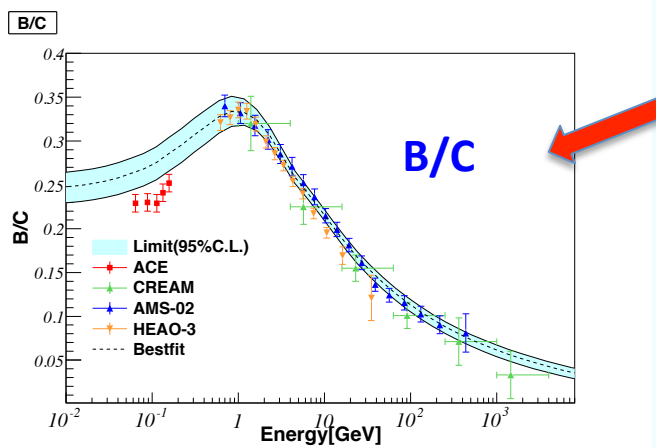

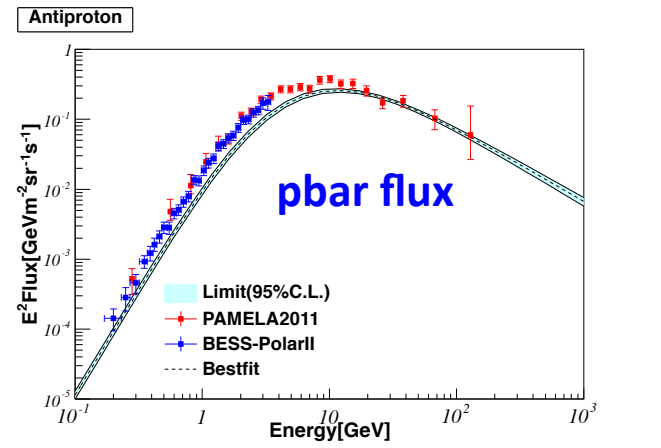

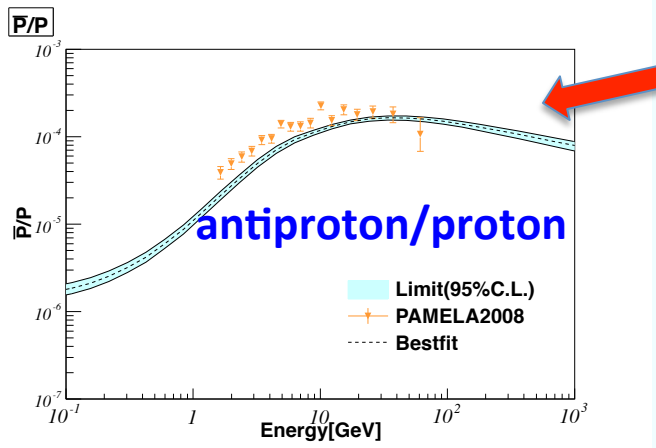

Best fits

AMS-02 data on proton flux and B/C ratio are well reproduced by the GALPROP diffusion reacceralation (DR) models Vc =0

Predictions

E>10 GeV: Antiproton fluxes are consistent with the PAMELA data
E < 10 GeV: 40% lower than the data of PAMELA and BESS-Polar II

Calculation of spectrum by using the parameters allowed within 95% CL

Construct sophisticated GALPROP models: (i) flattening of diffusion coefficient together with a convection term & a break in the injection spectrum; (ii) solar modulation have a charge sign dependence

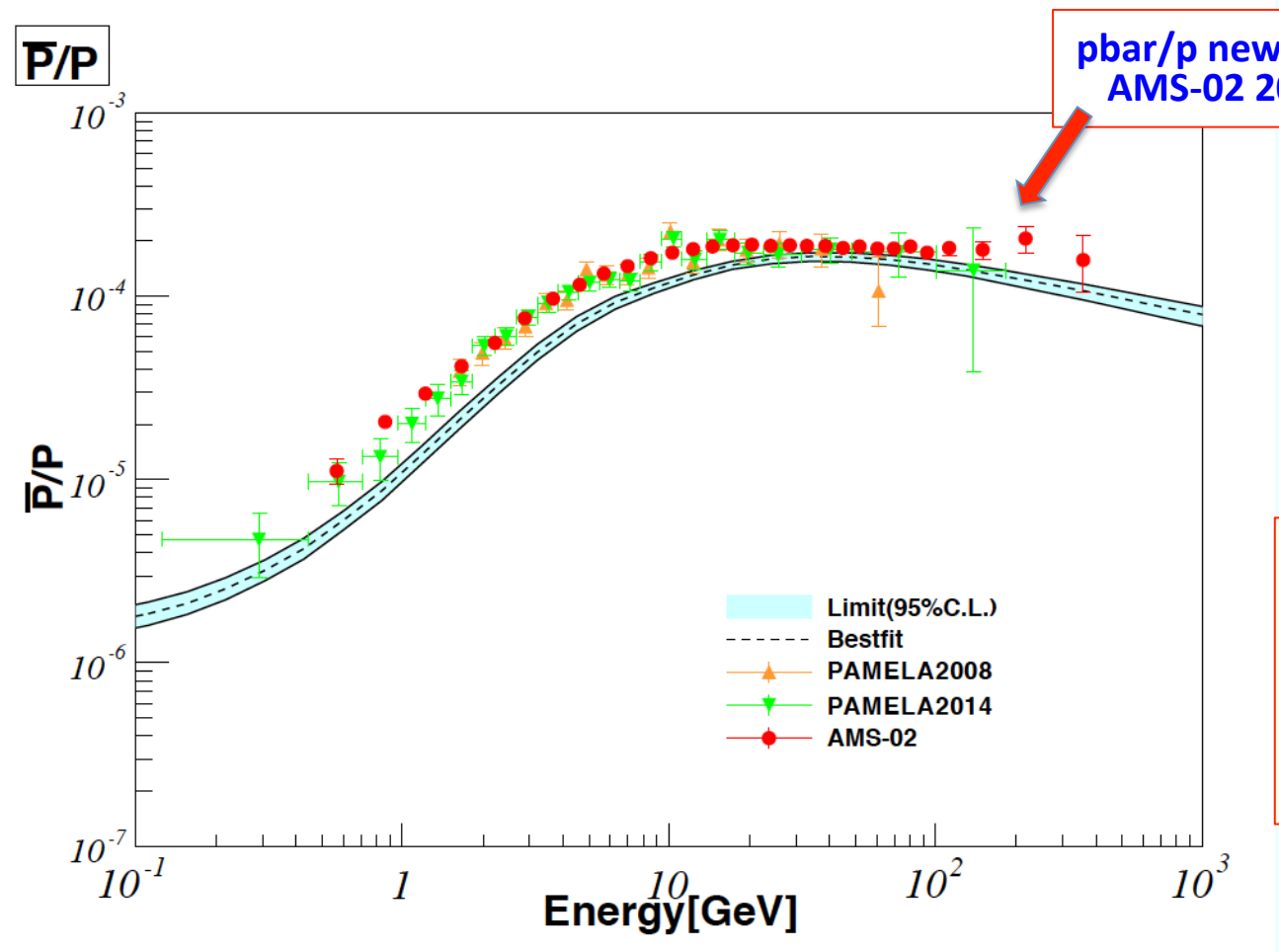

The AMS-02 pbar/p data are consistent with the background overall

In Donato et al. 2009 result based on the two-zone diffusion model actually underestimated the pbar at high energies.

Conclusion: our predictions and new data are highly consistent, except for a few data points at very high energies, which have relatively larger uncertainties. It is then crucial to make more precise measurements on this ratio at high energy region.

Uncertainties in Positron Backgrounds

Through scanning the whole parameter space allowed at 95%CL, the uncertainties of the backgrounds are obtained

Positron fraction

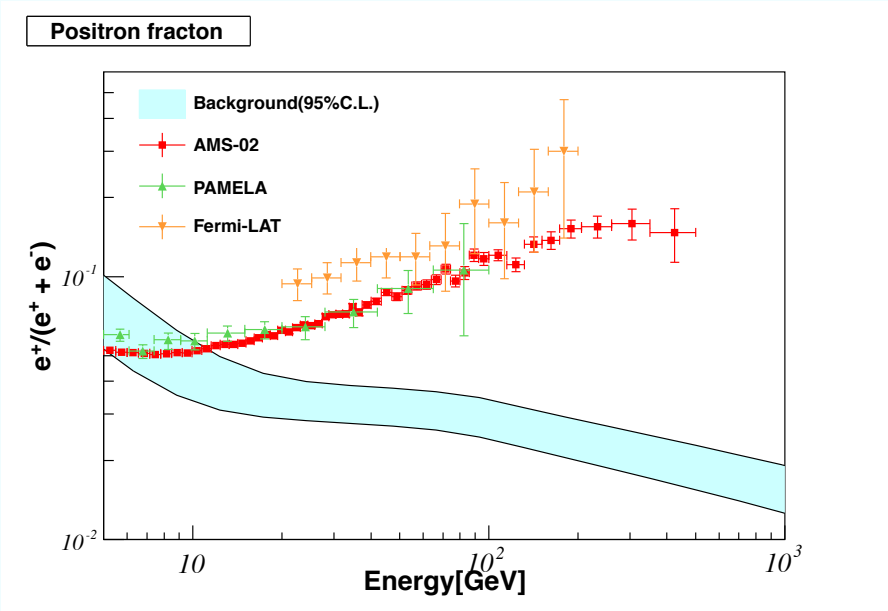

electron and positron fluxes

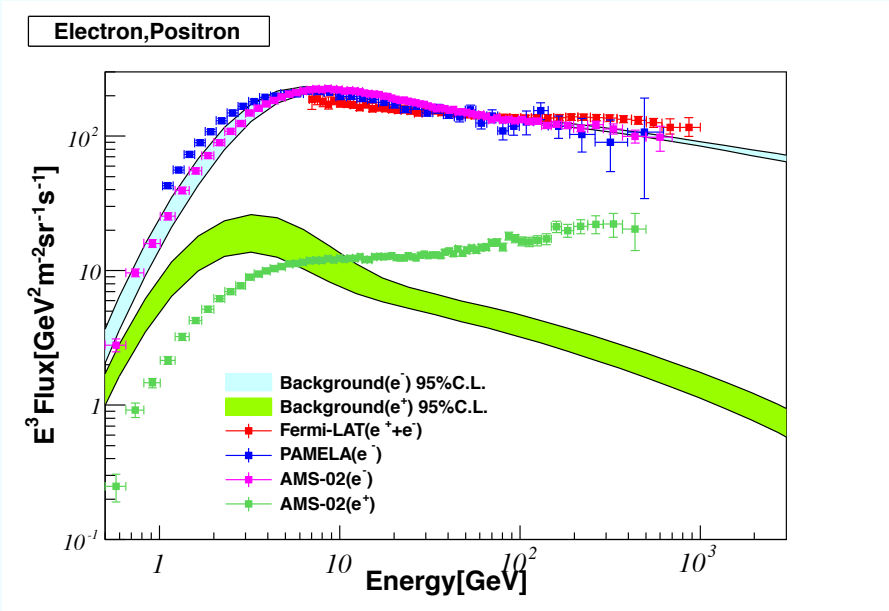

$$\rho_{e1} = 4 \text{ GV} \qquad \gamma_{e1} = 1.46,\ \gamma_{e2} = 2.72$$

$$\rho_{e2} = 86.8 \text{ GV} \qquad \gamma_{e3} = 2.49$$

Shaded bands for the variation of the propagation parameters within 95% CL. The uncertainties for positron reach a factor of 2

Predictions and Uncertainties in DM Annihilation

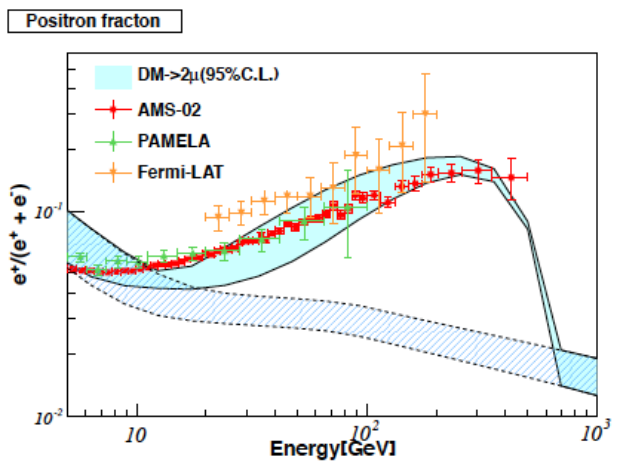

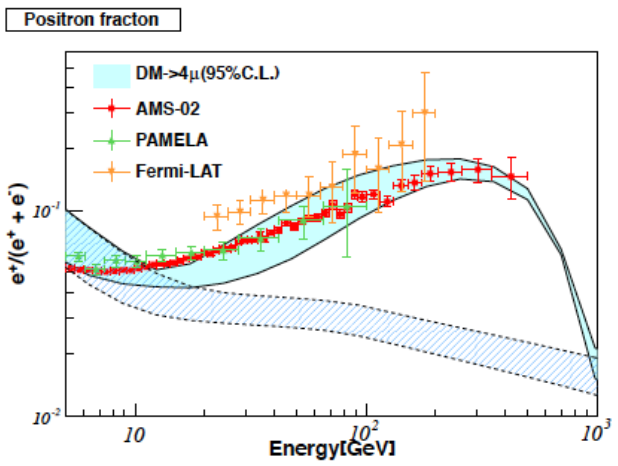

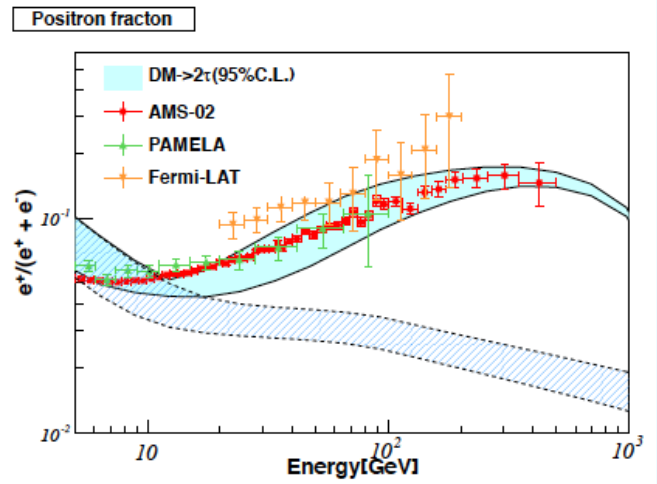

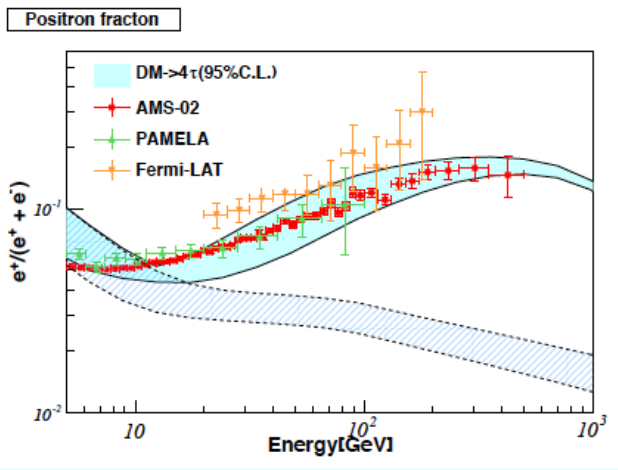

Best-fit values (2013)

$$2\mu : m_\chi = 570 \text{ GeV},$$
$$4\mu : m_\chi = 1.10 \text{ TeV},$$
$$2\tau : m_\chi = 1.5 \text{ TeV},$$
$$4\tau : m_\chi = 3.1 \text{ TeV},$$

$$\langle\sigma v\rangle = 6.7 \times 10^{-24} \text{ cm}^3\text{s}^{-1},$$
$$\langle\sigma v\rangle = 1.5 \times 10^{-23} \text{ cm}^3\text{s}^{-1},$$
$$\langle\sigma v\rangle = 5.3 \times 10^{-23} \text{ cm}^3\text{s}^{-1},$$
$$\langle\sigma v\rangle = 1.2 \times 10^{-22} \text{ cm}^3\text{s}^{-1}.$$

Hatched band for uncertainty of background at 95% CL

Best-fit values in 2013 data describe AMS-02 new data. Uncertainties within a factor of 2 for E < 500 GeV, and the uncertainties from background are much smaller for E>> 500

Predictions and Uncertainties in DM Annihilation

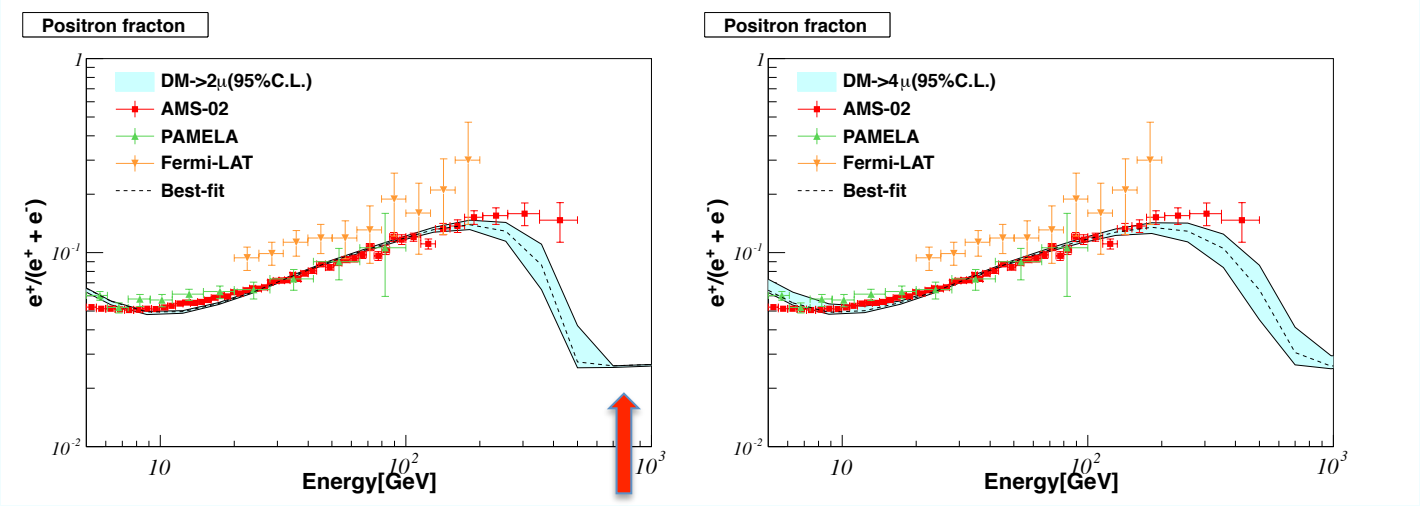

Uncertainties of background parameters and DM parameters are simultaneously considered

Predictions and Uncertainties in Antiproton Flux Resulting From DM Annihilation into bbbar

Consider reference propagation models: minimal, median and maximal fluxes

parameters	Min	Med	Max
$Z_h(\mathrm{kpc})$	1.8	3.2	6.0
D_0/Z_h	1.96	2.03	1.77
δ	0.30	0.29	0.29
$V_a(\mathrm{km}\cdot\mathrm{s}^{-1})$	42.7	44.8	43.4
γ_{p1}	1.75	1.79	1.81
γ_{p2}	2.44	2.45	2.46

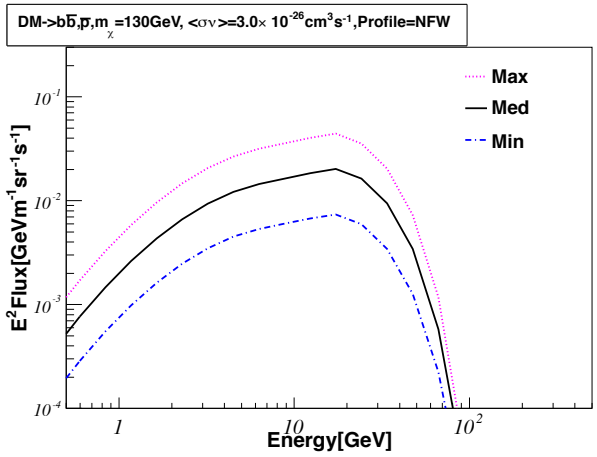

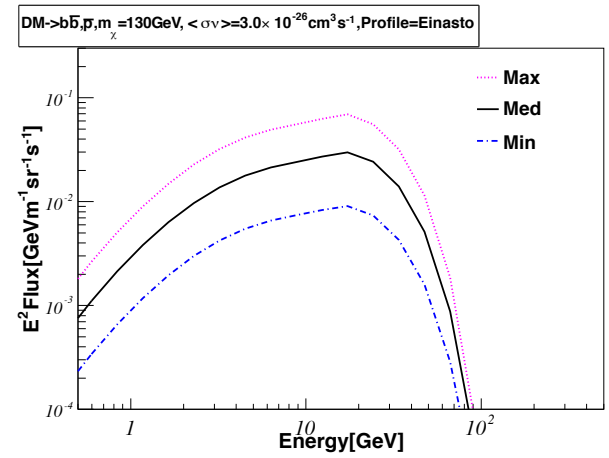

At 95% CL, the difference between min and max configuration is within O(10).

Previous analyses: uncertainties ~O(100), e.g. F.Donato, etal, astro-ph/0306207

By a factor of two among different profiles

Such a significant improvement due to precision AMS-02 data on B/C ratio

Upper limits on Cross Sections for DM Annihilation from PAMELA Antiproton Data

Global fit including PAMELA antiproton data

Method: Bayesian updating

$$P(\boldsymbol{\theta}', \boldsymbol{\theta}|D') = \frac{\mathcal{L}(D'|\boldsymbol{\theta}', \boldsymbol{\theta})\pi(\boldsymbol{\theta}')\tilde{\pi}'(\boldsymbol{\theta})}{\int \mathcal{L}(D'|\boldsymbol{\theta}', \boldsymbol{\theta})\pi(\boldsymbol{\theta}')\tilde{\pi}(\boldsymbol{\theta})d\boldsymbol{\theta}'d\boldsymbol{\theta}},$$

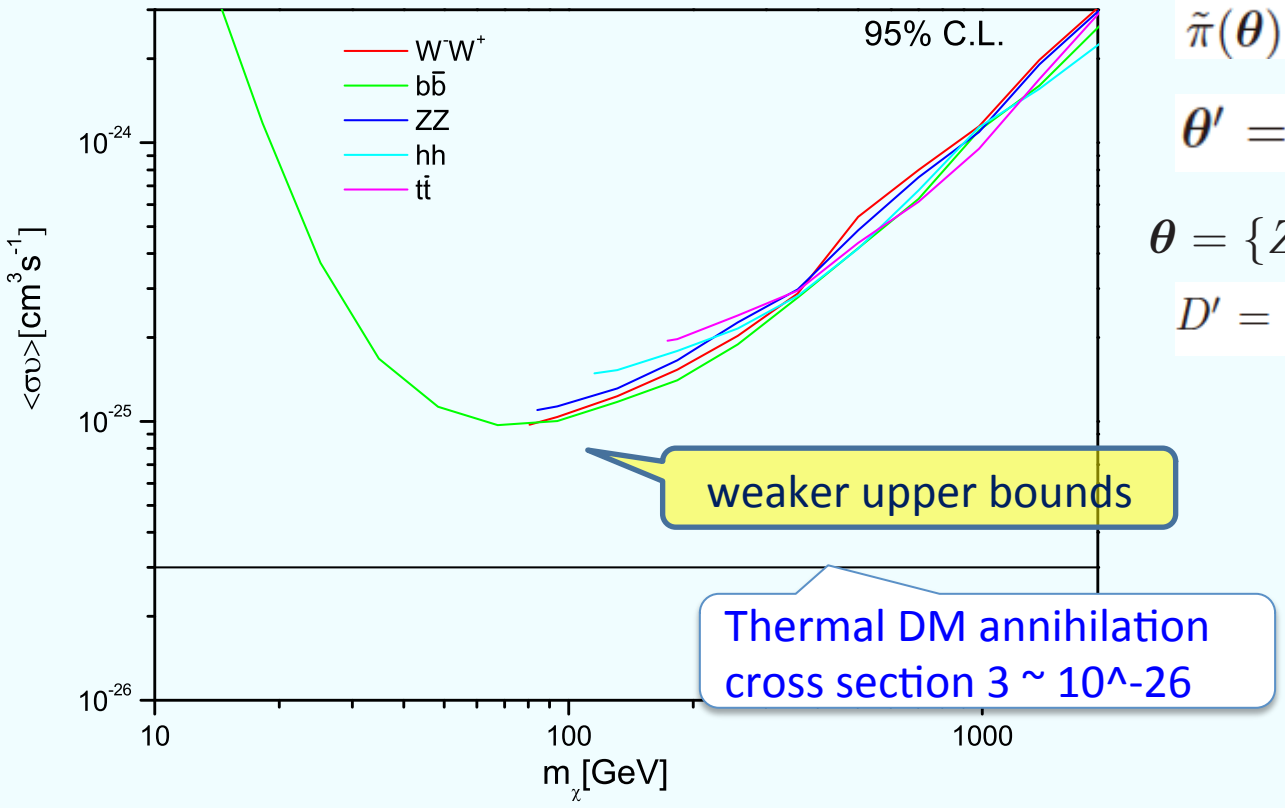

$$\tilde{\pi}(\boldsymbol{\theta}) = P(\boldsymbol{\theta}|D)$$

$$\boldsymbol{\theta}' = \{\langle\sigma v\rangle, m_\chi\}$$

$$\boldsymbol{\theta} = \{Z_h, D_0, \delta, V_a, \gamma_{p1}, \gamma_{p2}\}.$$

$$D' = \{D_p^{\rm PAM}, D_{\bar{p}/p}^{\rm PAM}\}$$

$$N_{q\bar{q}} = 2.97 \ (q = u, d),$$

$$N_{b\bar{b}} = 2.66, \ N_{t\bar{t}} = 3.20$$

$$N_{WW} = 1.42,$$

$$N_{ZZ} = 1.48,$$

$$N_{hh} = 2.18,$$

Considering the uncertainties in all the propagation parameters, the upper limits from PAMELA antiproton data are weakened by ~O(10)

Projection of AMS-02 Sensitivity on Antiproton

The reported new AMS-02 data on the antiproton flux is warmly welcome!

- **Expected number of antiproton for a given exposure time, and uncertainty**

$$N = \epsilon a(T_i)\phi(T_i)\Delta T_i \Delta t, \qquad \Delta N = \sqrt{N}. \qquad \Delta\phi(T_i)_{\rm sta} = \sqrt{\frac{\phi(T_i)}{\epsilon a(T_i)\Delta T_i \Delta t}}.$$

$$\Delta\phi(T_i) = \sqrt{\Delta\phi(T_i)^2_{\rm sta} + \Delta\phi^2_{\rm sys}}. \qquad \Delta\phi_{\rm sys} = 8\%.$$

Due to misidentification of background protons and electrons as antiprotons

- **Acceptance of antiproton at kinetic energy T and the efficiency of detector**

  a(T) =0.147 m^2 , (1– 11 GeV);

  a(T) =0.030 m^2, (11– 150 GeV); a(T) << 1, T >150

  ε=90%, (> 1 GeV)

- **Data binning, according to AMS-02 rigidity resolution and kinetic resolution**

$$\frac{\Delta R}{R} = 0.000477 \times R + 0.103. \qquad \frac{\Delta T}{T} = \left(\frac{T + 2m_p}{T + m_p}\right)\frac{\Delta R}{R},$$

AMS-02 Antiproton Mock Data (3-yr)

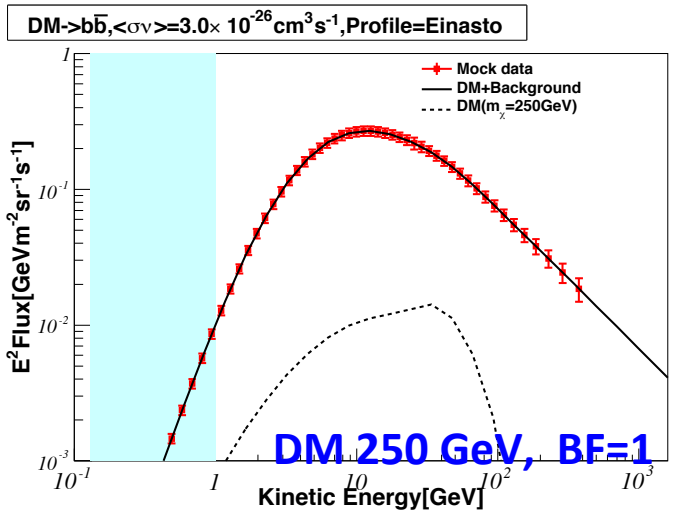

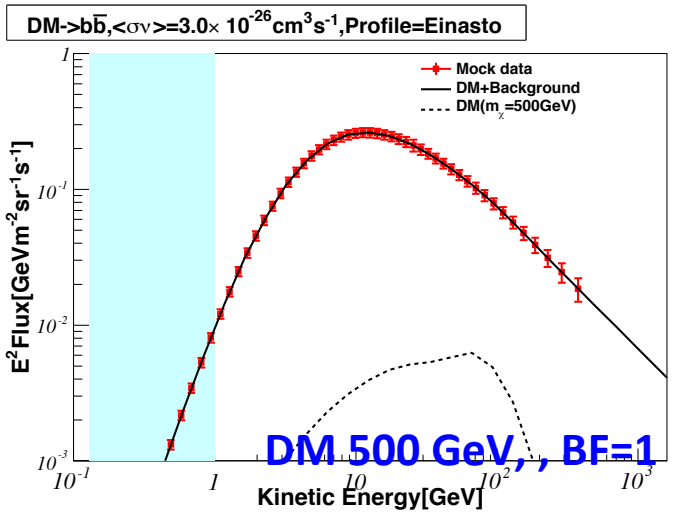

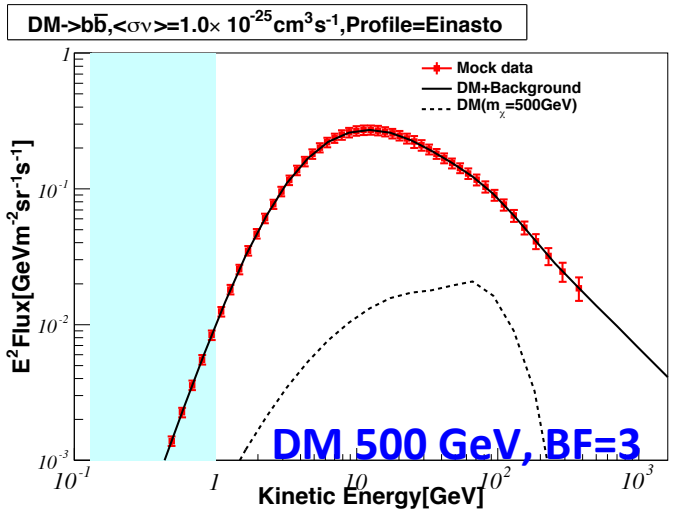

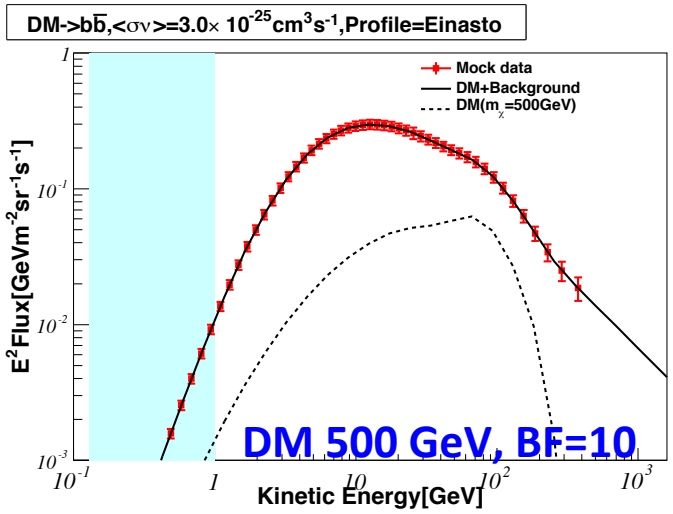

Dashed line represents the contribution from DM only

Solid line represents the sum of background and DM contribution

$$\langle \sigma v \rangle = \mathrm{BF} \times (3 \times 10^{-26} \mathrm{cm}^3 \mathrm{s}^{-1})$$

Halo DM profile: Einasto Profile

Antiproton background is generated according to the best-fit propagation parameters

Reconstruction of DM Properties

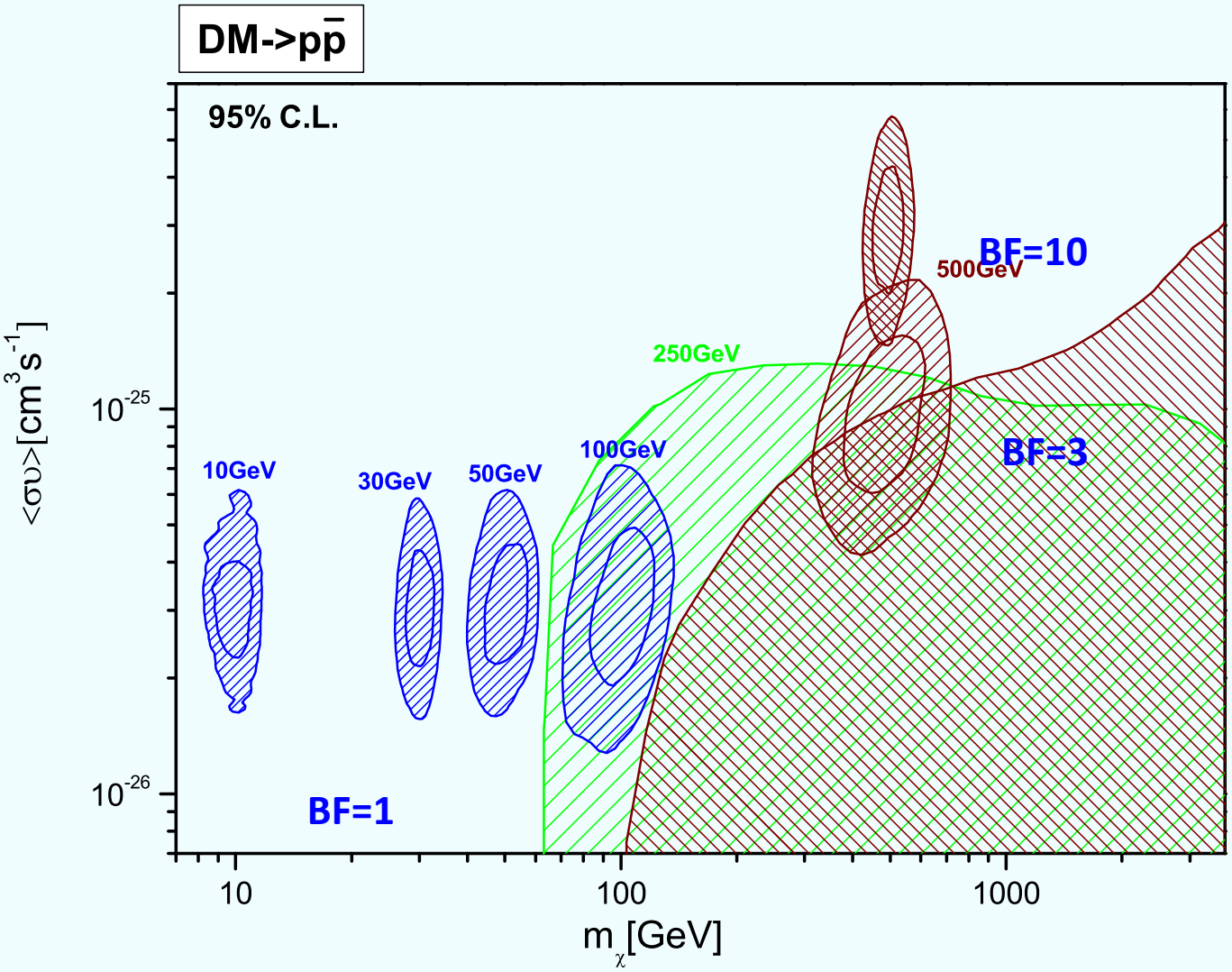

The cross section can be reconstructed within O(2), masses O(30%) at 95% CL for light DM (<100 GeV) and BF=1. Reconstruction is possible for heavy DM with large boost factor(BF)

Mechanisms for Boost Factor

The observed positron excesses contradict with thermal WIMP scenario.
Velocity (temperature)-dependent cross sections can solve the problem

1) Briet-Wigner resonance-enhancement

1) Resonance-enhancement

$$\sigma = \frac{16\pi}{E_{\rm cm}^2 \bar{\beta}_i \beta_i} \frac{M^2\Gamma^2}{(E_{\rm cm}^2 - M^2)^2 + M^2\Gamma^2} B_i B_f,$$

(E_{cm}^2-M^2)→ v^2

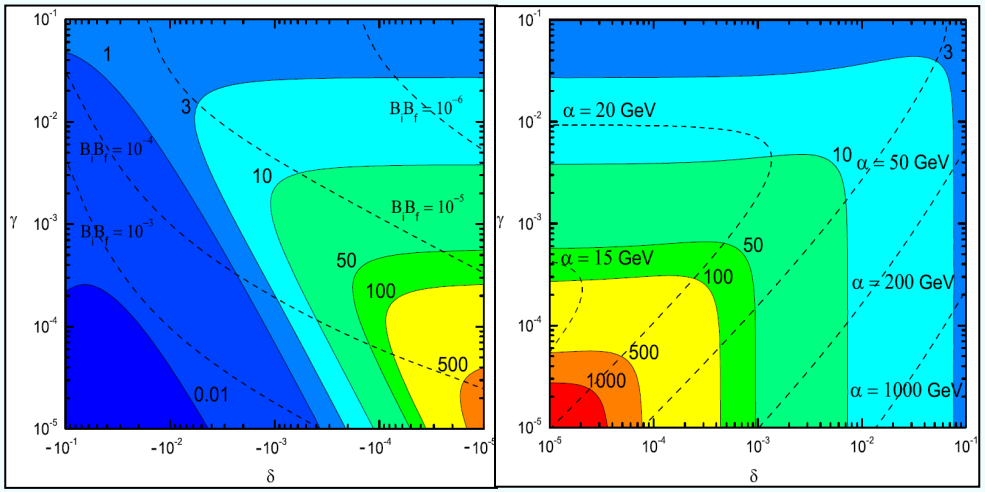

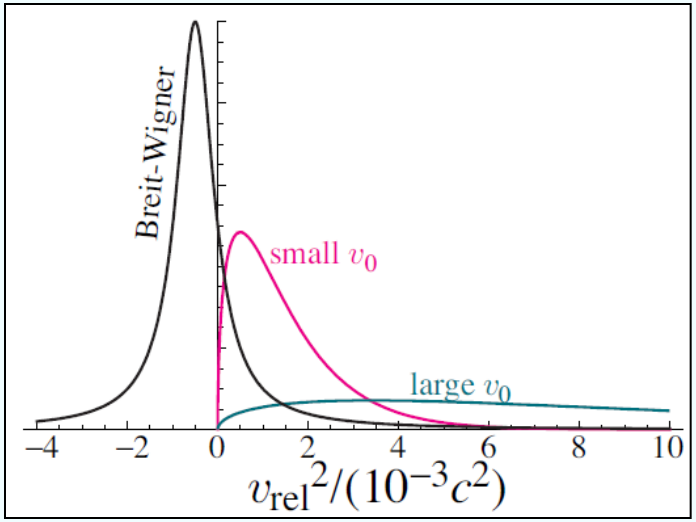

W.L. Guo, Y.L. Wu, PRD79,055012(2009)

Mechanisms for Boost Factor

2) DM conversion

DM conversion can provide a boost of DM relic density to compensate the large annihilation cross section

$$\chi_i\chi_i \leftrightarrow \chi_j\chi_j$$

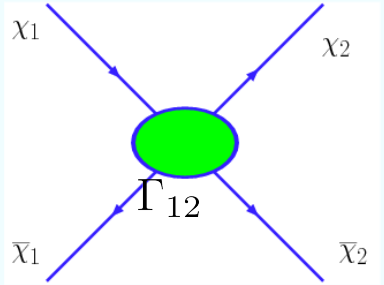

- Thermal evolution for interacting DM

$$\frac{x_i}{Y_{ieq}}\frac{dY_i}{dx_i} = -\frac{\Gamma_i}{H}\left(\frac{Y_i^2}{Y_{ieq}^2}-1\right)-\frac{\Gamma_{ij}}{H}\left(\frac{Y_i^2}{Y_{ieq}^2}-\frac{Y_j^2}{Y_{jeq}^2}\right)$$

- Boltzmann equation

$$\frac{dY_i(z)}{dz} = -\frac{\lambda}{z^2}\left[\langle\sigma_i v\rangle(Y_i^2-Y_{ieq}^2)-\sum_j\langle\sigma_{ij}v\rangle(Y_i^2-r_{ij}^2(z)Y_j^2)\right]$$

$$z \equiv m_1/T$$

$$\lambda \equiv zs/H = 0.263(g_{*s}/g_*^{1/2})m_1 m_{PL}$$

$$r(z)_{ij} = \left(\frac{g_i}{g_j}\right)\left(\frac{m_i}{m_j}\right)^{3/2}\exp\left[-(m_i-m_j)/T\right]$$

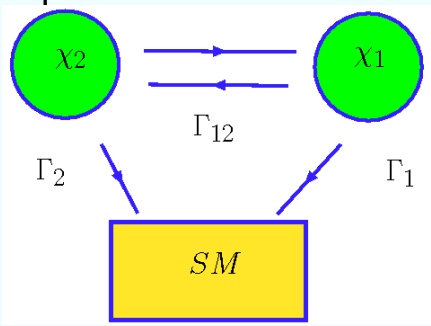

Z.P. Liu, Y.L. Wu, Y.F. Zhou, EPJC71,1749 (2011)

Thermal Evolution with DM Conversion

1. Thermal equilibrium with SM

$$Y_1 \approx Y_{1,eq},\ Y_2 \approx Y_{2,eq},\ \boxed{Y_2 \gg Y_1} \qquad (3 < z < z_{dec} \approx 25)$$

2. Decouple from SM, but still in equilibrium with each other

$$(z_{dec} < z < z_c \approx (\ln g)/\Delta)$$

$$Y_1 \neq Y_{1,eq},\ Y_2 \neq Y_{2,eq},\ \text{ but } Y_2/Y_1 \approx r(z)$$

3. Late time DM conversion at large z
   - Slow conversion characterized by r(z)
   - Crossing point $Y_2(z) = Y_1(z)$ near z_c
4. Complete decouple (freeze-out)

$$Y_1 = \text{const.}, Y_2 = \text{const.}, \boxed{Y_2 \ll Y_1}$$

Freeze-out condition

$$\frac{Y_2 \langle \sigma_{12} v \rangle}{H} < 1$$

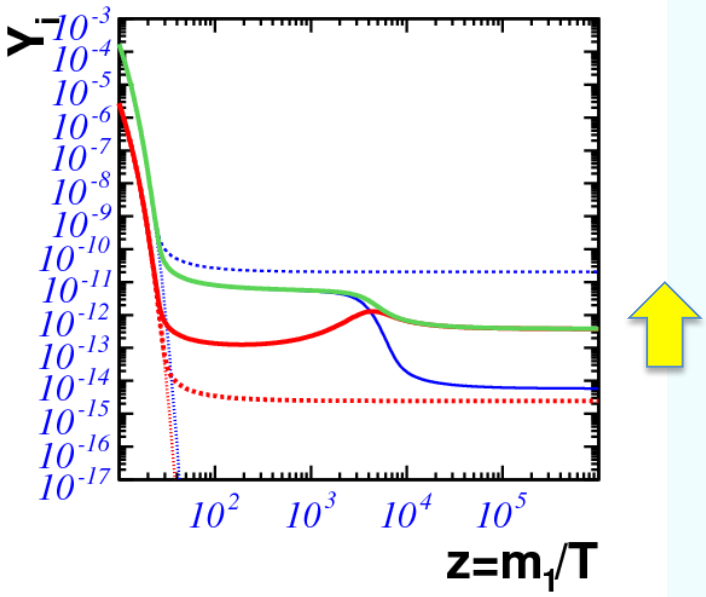

Y1(z) increased eventually

Z.P. Liu, Y.L. Wu, Y.F. Zhou, EPJC71,1749 (2011)

3) Sommerfeld Enhancement (Explain AMS02 ?)

The Sommerfeld enhancement of DM particle annihilation cross section occurs when the annihilating particles self-interact through a long-range attractive potential V (r) at low relative velocities, which causes the distortion of the wave function at the origin

The effect of the Sommerfeld enhancement and the constraint from thermal relic density depend on the nature of the force-carrier particle

i) vector force-carrier case

For force-carrier being a vector boson, the induced long-range potential is of Yukawa type, the process of DM annihilation into force carries is an s-wave process

$$(\sigma_{2\phi} v_{\rm rel})_0^{\rm vector} = \frac{\pi\alpha^2}{m_\chi^2}.$$

In marginal agreement with AMS-02

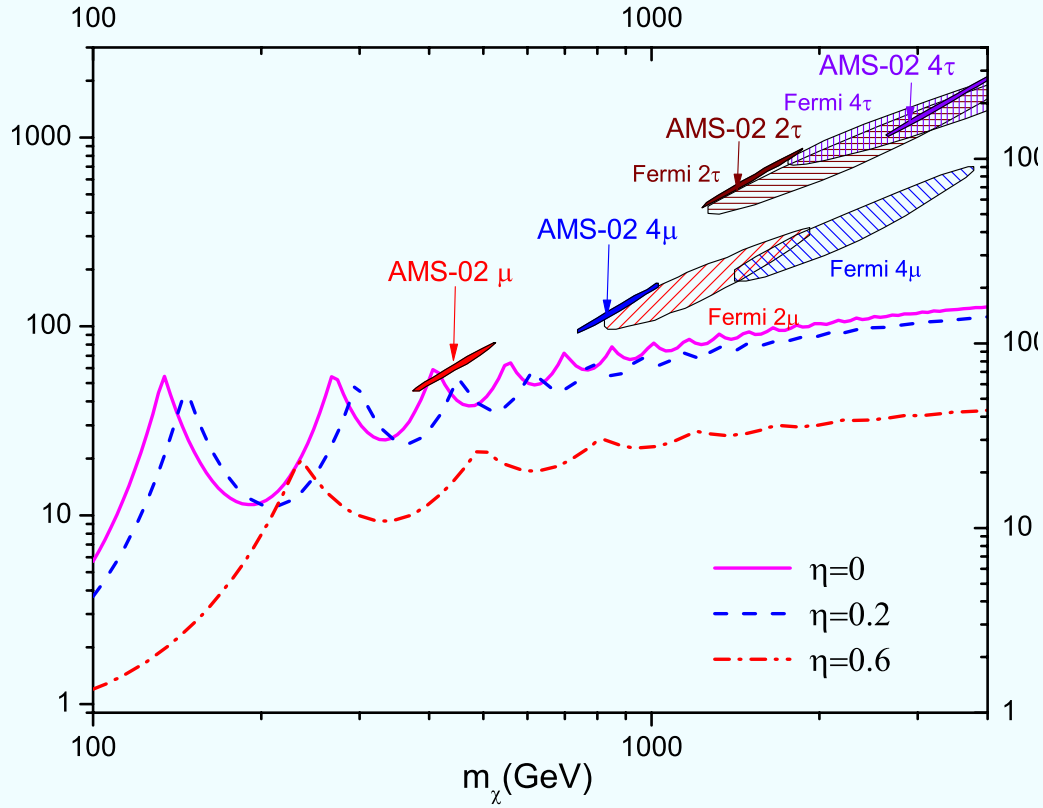

Z.P.Liu, Y.L. Wu, Y.F. Zhou, arXiv:1305.5438, PRD

3) Sommerfeld Enhancement (Explain AMS02 ?)

ii) Scalar force-carrier case

$$(\sigma_{2\phi} v_{\rm rel})_0^{\rm scalar} = \frac{3\pi\alpha^2 v_{\rm rel}^2}{8m_\chi^2}.$$

If the force carrier is a scalar, the same process becomes a velocity-suppressed p-wave process, which resulting in a weaker constraint. It is larger by a factor of 2.

In marginal agreement with AMS-02

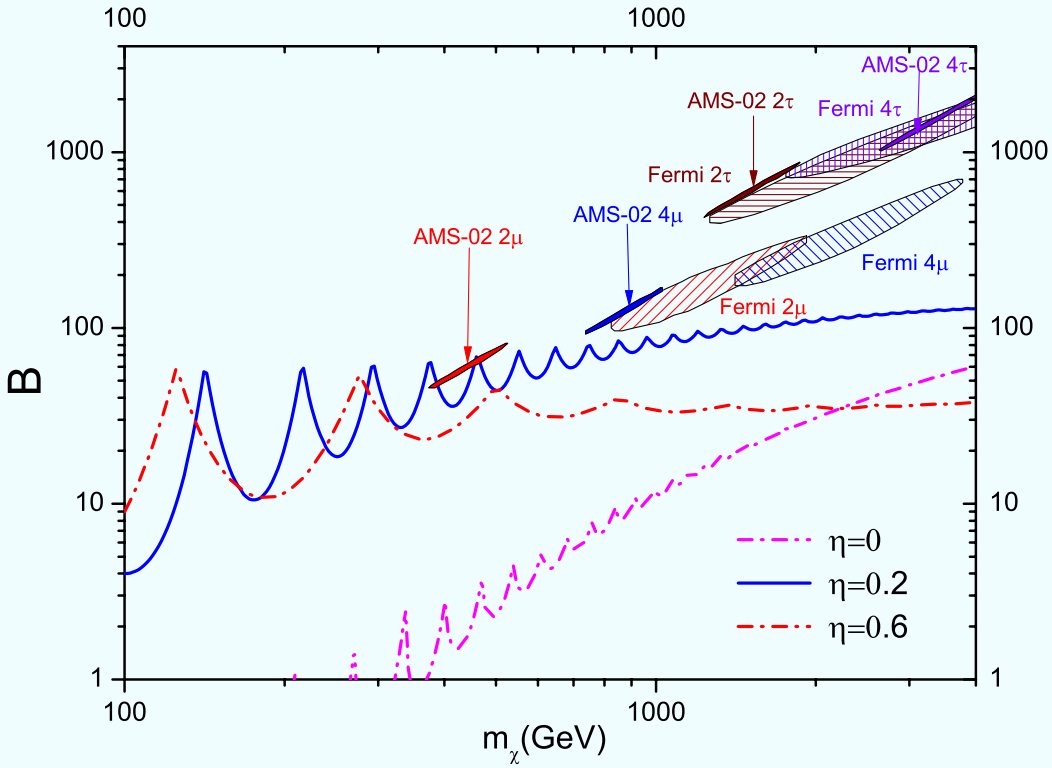

Z.P.Liu, Y.L. Wu, Y.F. Zhou, arXiv:1305.5438, PRD

3) Sommerfeld Enhancement (Explain AMS02)

iii) Pseudoscalar force-carrier

$$(\sigma_{2\phi} v_{\rm rel})_0^{\rm pseudoscalar} = \frac{\pi \alpha^2 v_{\rm rel}^2}{24 m_\chi^2}.$$

If the force carrier is a pseudoscalar, the induced long-range potential is a tensor force, and the process of DM annihilation into force carries is again a p-wave process. Much larger enhancement can be obtained in the resonance region!

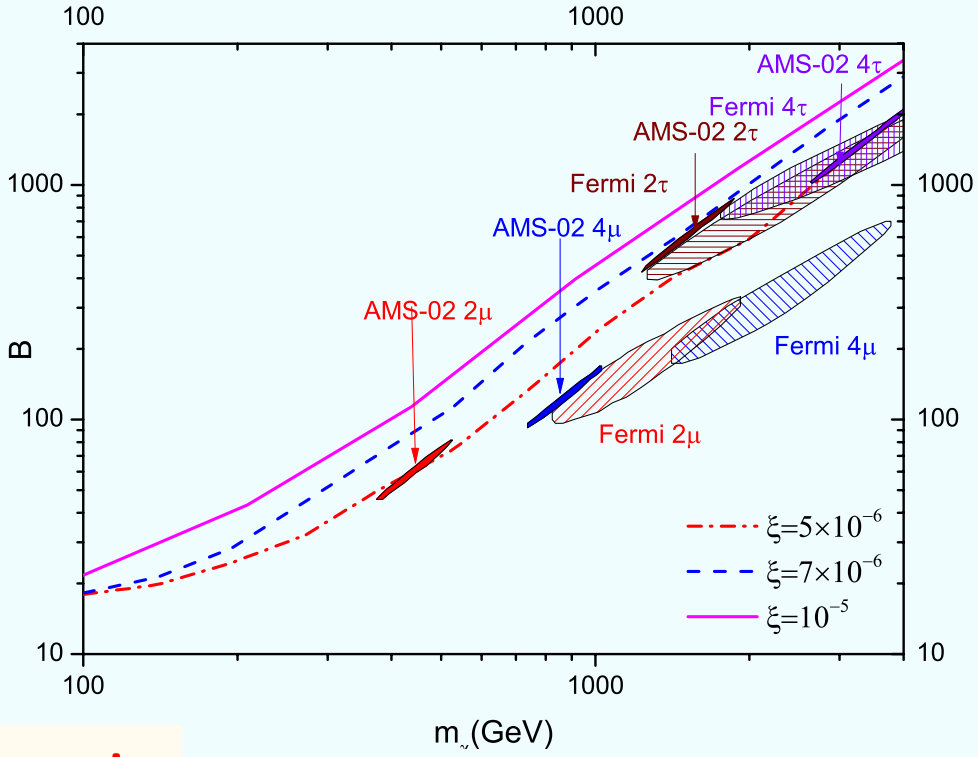

In better agreement with AMS-02

Conclusion: the Sommerfeld enhancement is still a viable mechanism to account for the current cosmic-ray lepton anomalies

Z.P.Liu, Y.L. Wu, Y.F. Zhou, arXiv:1305.5438, PRD

CONCLUSIONS

- Accurate prediction for DM-induced CR signals requires better understanding of the propagation of CR particles.
- Precision AMS-02 data provide us rich information, and enable us to distinguish different DM models. The data favor DM annihilation over DM decay.
- Precision AMS-02 data alone (B/C ratio + proton flux) allow us to determine more precisely the major CR propagation parameters, e.g. the uncertainty in D0/Zh is within 5%.
- The uncertainties in positron fraction are constrained to be O(2), and that in antiproton be O(10), both are significantly smaller than the analyses prior to AMS-02 [O(10), O(100)]
- The projection for AMS-02 sensitivity on antiproton flux,

  for DM E<200 GeV with thermal σv, the cross section can be reconstructed within O(2) for 3-year data taking.
- More precise measurements on the high energy region will be crucial for a better understanding on CRs and DM

THANKS

谢谢！